Journal of Medicinal Chemistry

Article

pubs.acs.org/jmc

Discovery of an Orally Efficacious Inhibitor of Anaplastic Lymphoma Kinase

Diane E. Gingrich,* Joseph G. Lisko, Matthew A. Curry, Mangeng Cheng, Matthew Quail, Lihui Lu, Weihua Wan, Mark S. Albom, Thelma S. Angeles, Lisa D. Aimone, R. Curtis Haltiwanger, Kevin Wells-Knecht, Gregory R. Ott, Arup K. Ghose, Mark A. Ator, Bruce Ruggeri, and Bruce D. Dorsey

Worldwide Discovery Research, Cephalon, Inc., 145 Brandywine Parkway, West Chester, Pennsylvania 19380, United States

Supporting Information

ABSTRACT: Anaplastic lymphoma kinase (ALK) is a promising therapeutic target for the treatment of cancer, supported by considerable favorable preclinical and clinical activities over the past several years and culminating in the recent FDA approval of the ALK inhibitor crizotinib. Through a series of targeted modifications on an ALK inhibitor diaminopyrimidine scaffold, our research group has driven improvements in ALK potency, kinase selectivity, and overall pharmaceutical properties. Optimization of this scaffold has led to the identification of a potent and efficacious inhibitor of ALK, **25b**. A striking feature of **25b** over previously described ALK inhibitors is its >600-fold selectivity over insulin receptor (IR), a closely related kinase family member. Most importantly, **25b** exhibited dose proportional escalation in rat compared to compound **3** which suffered dose limiting absorption preventing further advancement. Compound **25b** exhibited significant in vivo antitumor efficacy when dosed orally in an ALK-positive ALCL tumor xenograft model in SCID mice, warranting further assessment in advanced preclinical models.

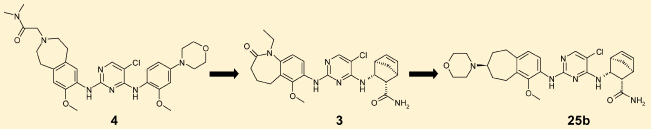

INTRODUCTION

Despite progress made in the past decade, lung cancer continues to be the most frequent cause of cancer-related deaths among men and women worldwide with greater than 200 000 new cases estimated this year in the United States alone.[1] One area of great promise in the treatment of lung and other cancers has been the advent of targeted kinase therapies.[2] The identification of genetic modifications resulting in tumor development has provided an opportunity to target specific kinases with the goal of providing more beneficial chemotherapeutic agents.[3] One kinase that has garnered increasing attention as a therapeutic target is anaplastic lymphoma kinase (ALK) as illustrated by its growing pharmaceutical interest[4] and its role in non-small-cell lung cancer (NSCLC).[5] ALK is a receptor tyrosine kinase (RTK) member of the insulin receptor (IR) superfamily, originally identified as part of the NPM-ALK fusion gene in anaplastic large cell lymphoma (ALCL) with a t(2;5) chromosomal translocation.[6] While the physiological role of ALK receptor has not been well-defined, involvement of ALK in the oncogenesis of various human cancers has been well documented and characterized. Besides NPM-ALK, various other ALK fusion genes were subsequently detected in ALCLs, inflammatory myofibroblastic tumor, diffuse large B-cell lymphoma, systemic histiocytosis, and most notably, NSCLC, resulting in the generation of oncogenic ALK fusion proteins with constitutive phosphorylation/activation of ALK.[7] The constitutive kinase activity associated with ALK fusions appears to play an essential role in proliferation and survival of human cancer cells.[8] Recently, it has also been reported that germline mutations in ALK are the cause of most hereditary neuroblastoma cases, and ALK activation by mutation and/or gene amplification is functionally relevant in high-risk sporadic neuroblastoma.[9] The dysregulated signaling resulting from these rearrangements or mutations/gene amplification has led to a state of "oncogenic addiction", providing an opportunity for intervention with small molecule inhibitors.[10]

Crystal structures have been solved for the unphosphorylated catalytic domain of ALK complexed with two ATP-competitive inhibitors.[11] This structural information can be parlayed into the design of additional ALK inhibitors and also provides insight into the basis for activation of ALK by the active site mutations observed in neuroblastoma. Pfizer's PF-02341066 (crizotinib, **1**),[12] a dual ALK/cMET inhibitor, was the first ALK inhibitor advanced into clinical trials and more recently received FDA approval for treatment of patients with locally advanced or metastatic ALK-positive NSCLC.[13,14] Other pharmaceutical companies have also been active in the ALK arena exploring an array of varied scaffolds. Novartis specifically has published patent applications around a diaminopyrimidine scaffold, as well as describing extensive pharmacology associated with a lead compound NVP-TAE684 (**2**).[15] In addition, several groups have reported tyrosine kinase inhibitors which overcome crizotinib resistance.[16]

Our research efforts have focused on developing potent and selective inhibitors of ALK with modifications to the diaminopyrimidine scaffold, focusing on two major regions of the molecule designated as the A- and C-rings (Figure 2). Previously published research from our group identified a bicyclo[2.2.1]hept-5-ene ring system of compound **3** (Figure 1)

Received: November 16, 2011
Published: May 7, 2012

dx.doi.org/10.1021/jm201550q | J. Med. Chem. 2012, 55, 4580–4593

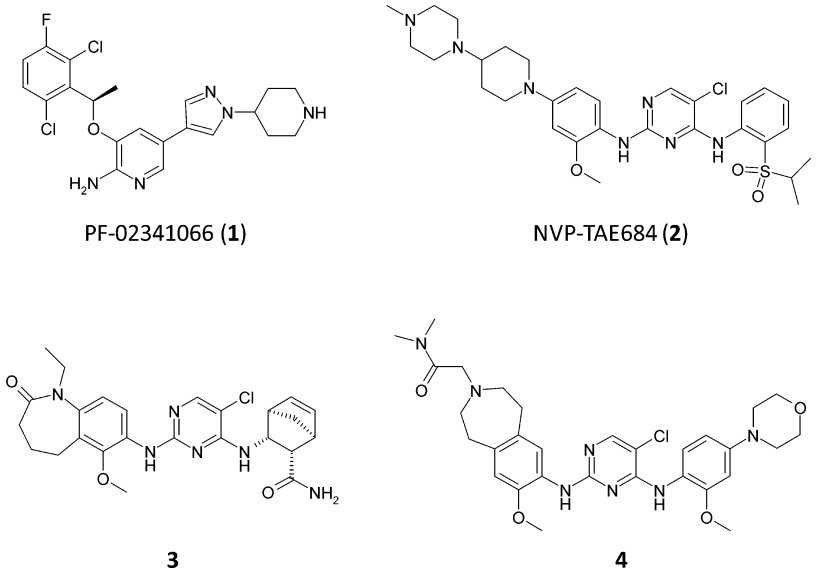

Figure 1. Small molecule ALK inhibitors.

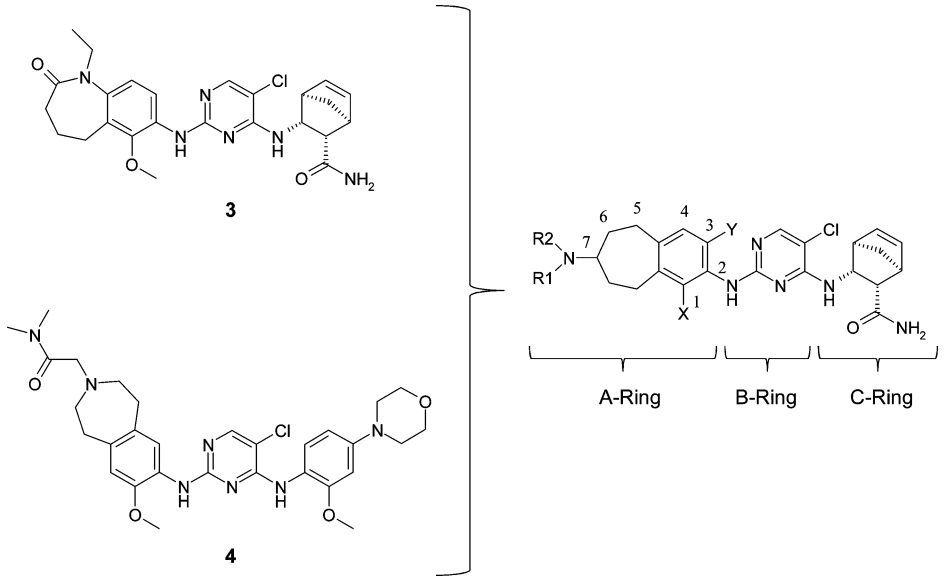

Figure 2. Optimization strategy and areas of modification on the diaminopyrimidine core.

as an alternative C-ring fragment impacting selectivity toward IR.[17] Our earlier report also highlighted that minor modifications to the A-ring fragment can impact IR/ALK selectivity. The combination of an A-ring methoxy selectivity determinant combined with the [2.2.1] C-ring system provided improved kinase selectivity observed with **3** versus other published inhibitors. Selectivity toward IR is of particular interest because of the involvement of IR in the regulation of glucose transport and glycogen and fat biosynthesis.[18,19] Avoiding potential complications from this activity was a major objective in designing second generation molecules with improved IR/ALK selectivity over initial lead compound **3**. While compound **3** provided a balanced profile consisting of ALK potency and global kinase selectivity, the modest IR/ALK selectivity led the team to optimize the diaminopyrimidine series further in an effort to improve selectivity toward IR (enzymatic IR/ALK IC_{50} ratio of >100). In addition, compound **3** lacked the ability to be dose escalated in preclinical toxicological species, precluding its further development (Table 4).

Compound **4** (Figure 1) was also previously identified by our group as an analogue with potent in vitro ALK activity but with a potential hERG liability, as indicated by an in vitro IC_{50} of 3.9 μM for hERG in a patch clamp assay (Supporting Information). The 2,3,4,5-tetrahydro-1*H*-benzo[*d*]azepine A-ring motif of **4** resulted in potent ALK inhibition while providing a site for functional group manipulation to balance potency with favorable physicochemical properties. A variety of substituents incorporated on the azepine nitrogen yielded changes in both the enzyme and cell inhibition, depending on the nature of the substituent. In an attempt to further modulate the potency and selectivity differences observed with the azepine analogues, the basic nitrogen was moved outside the seven-membered ring, resulting in an aminobenzocycloheptene motif (Figure 2). The resulting strategy was to identify suitable azepine or azepinone A-ring replacements to combine with the previously established bicyclo[2.2.1]hept-5-ene ring system, which would provide potent ALK inhibition, improved selectivity against the IR receptor and dose proportional increases in preclinical toxicology species.

dx.doi.org/10.1021/jm201550q | *J. Med. Chem.* 2012, 55, 4580–4593

Scheme 1. Synthesis of 7-Aminosubstituted 1-Methoxy-6,7,8,9-tetrahydro-5*H*-benzocycloheptene Amine Fragments[a]

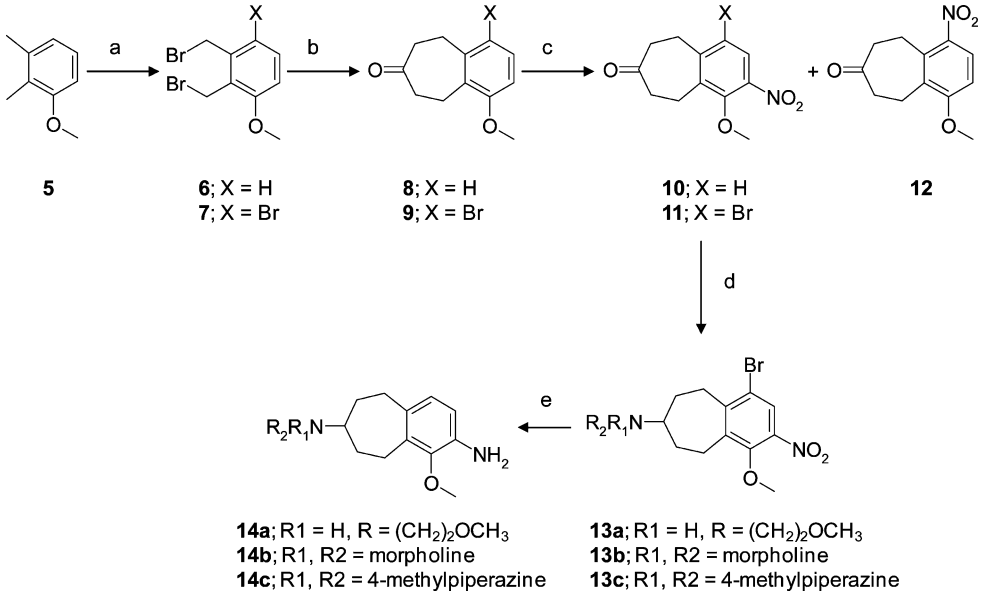

[a]Reagents and conditions: (a) NBS [2 equiv (X = H); 3 equiv (X = Br)], AIBN, CCl_4, 80−99%; (b) (i) 3-oxopentanedioic acid diethyl ester, 0.6 M sodium bicarbonate, tetra-*n*-butylammonium iodide, methylene chloride, 24 h; (ii) 1 M KOH, EtOH, reflux 3 h; 33% over two steps; (c) KNO_3, $(CF_3CO)_2O$, CH_3CN, 53% (d) $NaBH(OAc)_3$, amine, acetic acid, CH_2Cl_2, 44−70%; (e) H_2, Pd/C wet, ethanol, 93%.

Scheme 2. Synthesis of 7-Aminosubstituted 3-Methoxy-6,7,8,9-tetrahydro-5*H*-benzocycloheptene Amine Fragments[a]

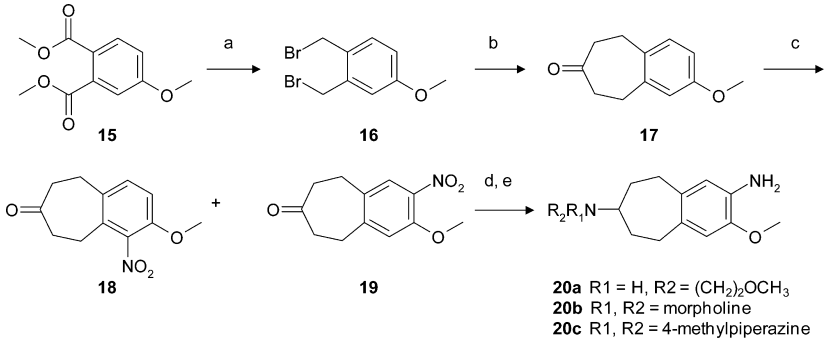

[a]Reagents and conditions: (a) (i) $LiAlH_4$, THF, 0 °C, 65−97%; (ii) PBr_3, CH_2Cl_2, 62−94%; (b) (i) 3-oxopentanedioic acid diethyl ester, 0.6 M sodium bicarbonate, tetra-*n*-butylammonium iodide, CH_2Cl_2, 24 h; (ii) 1 M KOH, EtOH, reflux 3 h, 50% over two steps (c) KNO_3, CH_3CN, 53−83%; (d) $NaBH(OAc)_3$, amine, acetic acid, CH_2Cl_2, 65−90%; (e) H_2, Pd/C wet, ethanol, 85−95%.

A focused medicinal chemistry effort evaluating modifications to the aminobenzocycloheptene ring system was therefore initiated.

CHEMISTRY

Two differentially substituted methoxy A-ring fragments were prepared to assess the impact of the methoxy group at the C1 versus C3 position of the A-ring on ALK potency and selectivity for ALK versus IR. The initial synthesis of 1-methoxy-6,7,8,9-tetrahydro-5*H*-benzocyclohepten-2-ylamines (**14a−c**) outlined in Scheme 1 involved bromination of 1-methoxy-2,3-dimethylbenzene with *N*-bromosuccinimide (NBS) in carbon tetrachloride using either 2,2′-azo-bis-isobutyronitrile, benzoyl peroxide, or ultraviolet light as the initiator to give initial intermediate **6**. Conversion of **6** to the seven-membered ring **8** was accomplished using 3-oxopentanedioic acid diethyl ester in a biphasic reaction of methylene chloride and 0.6 M aqueous sodium bicarbonate with tetra-*n*-butylammonium iodide as a phase transfer catalyst. The resultant product was carried on without further purification and treated with potassium hydroxide in refluxing ethanol for 3 h to effect ester hydrolysis and decarboxylation. Nitration of **8** was achieved with potassium nitrate, trifluoroacetic anhydride in acetonitrile to give two nitration products, **10** and **12**, in a 1.3:1 ratio, which were separable with normal phase chromatography. Compounds **10** and **12** were versatile intermediates that allowed the introduction of chemical diversity through reductive amination chemistry. Compounds possessing the 2-amino-1-methoxy-5,6,8,9-tetrahydro-7-aminobenzocycloheptene fragment, as illustrated by compound **10**, provided better ALK inhibition compared to the corresponding regiomeric 1-amino-4-methoxy-5,6,8,9-tetrahydro-7-aminobenzocycloheptenane, **12**. As a result, only reductive alkylation products with 2-amino-1-methoxy A-ring substitution were pursued. The aminated products **13a−c** were subjected to hydrogenation conditions to provide the respective anilines in good yield.

A potential liability with the previously described synthetic pathway was the poor selectivity observed under the nitration conditions. To improve the overall yield of the desired nitration

dx.doi.org/10.1021/jm201550q | *J. Med. Chem.* 2012, 55, 4580−4593

Scheme 3. A- and C-Ring Coupling Sequence[a]

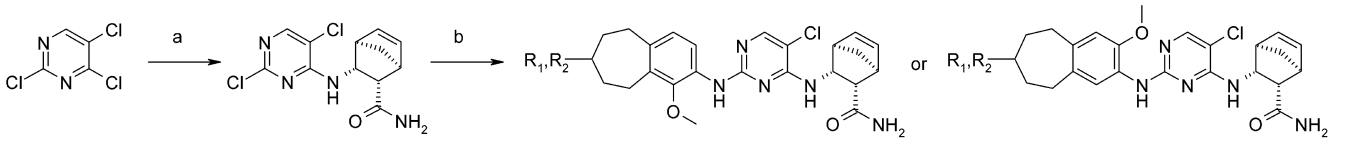

[a]Reagents and conditions: (a) K_2CO_3, (1*S*,2*S*,3*R*,4*R*)-3-aminobicyclo[2.2.1]hept-5-ene-2-carboxylic acid amide, DMF; (b) HCl, 2-methoxyethanol, substituted aminobenzocycloheptene A-ring fragment, 130 °C.

Table 1. ALK Inhibition Data for Select Diaminopyrimidine Analogues

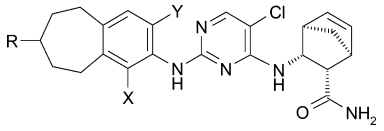

compd[a]	R	X	Y	ALK IC_{50}, nM[b]	Karpas-299 cell IC_{50}, nM	IR/ALK enzyme IC_{50} ratio	*S*(90)
3				14 ± 3	45	43	0.11
4				4 ± 1	30	345	0.03
23a	$MeO(CH_2)_2NH$-	OCH_3	H	21 ± 11	65	103	0.22
23b	$MeO(CH_2)_2NH$-	OCH_3	H	9 ± 1	30	>333	0.31
24a	$MeO(CH_2)_2NH$-	H	OCH_3	4 ± 2	40	46	0.23
24b	$MeO(CH_2)_2NH$-	H	OCH_3	11 ± 3	65	67	0.09
25a	morpholino-	OCH_3	H	35 ± 11	120	>29	0.15
25b	morpholino-	OCH_3	H	1.9 ± 0.5	20	662	0.14
26a	morpholino-	H	OCH_3	6 ± 1	40	88	0.21
26b	morpholino-	H	OCH_3	16 ± 5	120	77	0.04
27a	4-methylpiperazinyl-	OCH_3	H	16.2 ± 0.8	200	151	NT[c]
27b	4-methylpiperazinyl-	OCH_3	H	3.1 ± 0.3	20	>320	NT[c]
28a	4-methylpiperazinyl-	H	OCH_3	17 ± 5	150	>59	0.15
28b	4-methylpiperazinyl-	H	OCH_3	15 ± 6	150	>67	0.03

[a]Compounds designated "a" are the first eluting diastereomer and those designated "b" are the second eluting diastereomer from a reverse phase preparative HPLC column. [b]Average ± standard deviation of four or more determinations [c]NT, not tested.

product, the C-6 position was temporarily blocked with bromine as outlined in Scheme 1 (X = Br). Treatment of **5** with 3 equiv of NBS yielded the tribrominated product **7**. Ring annulation proceeded as previously described, and with the position para to the methoxy group blocked, nitration occurred ortho to the methoxy group to provide isomer **11** in good yield. Desired reductive aminations then yielded nitro intermediates **13a–c**, whose nitro groups were subsequently reduced to their corresponding anilines under standard Pd/C hydrogenation conditions, with concomitant reduction of the bromide to give **14a–c**.

As illustrated in Scheme 2, the regiomeric methoxy A-ring, 3-methoxy-6,7,8,9-tetrahydro-5*H*-benzocycloheptene-2,7-diamine, was prepared starting with 4-methoxyphthalic acid dimethyl ester (**15**). Bromination using phosphorus tribromide in methylene chloride provided **16**. The 6/7-fused ring system was formed in the same manner as previously outlined. Nitration of **17** yielded two nitrated products, **18** and **19**, in roughly a 1:1.6 ratio, respectively, which were separated on silica gel. Ketone **19** was subjected to reductive alkylation conditions with a select number of amines followed by hydrogenation to reduce the nitro group to the corresponding anilines (**20a–c**). A small number of analogues were prepared with the A-ring derived from compound **18** to evaluate potential potency differences between the A-ring methoxy regiomers. A 100-fold loss of ALK potency was observed with analogues resulting from **18** compared to regiomer **19**. As a result, efforts were focused on elaborating compound **19** with a diverse set of substituents.

The target analogues were assembled using our previously published chemistry involving tandom nucleophilic aromatic substitution reactions as shown in Scheme 3.[15] The (1*S*,2*S*,3*R*,4*R*)-3-aminobicyclo[2.2.1]hept-5-ene-2-carboxylic acid amide fragment is installed first on the 2,4,5-trichloropyrimidine. The appropriately substituted aminobenzocycloheptene ring fragment was subsequently incorporated to afford the fully assembled diaminopyrimidine scaffold. Noteworthy, analogues **23–28** were generated as diastereomeric pairs from racemic anilines **14** and **20**. Fortunately, the diasteromeric pairs were easily separated via preparative reverse phase HPLC.

RESULTS

ALK enzyme and cellular inhibition data, as well as IR enzyme inhibition data, were obtained for the above-described diasteriomeric pairs of targets as shown in Table 1.[20] Several trends were identified when evaluating the diastereomeric pairs comprised of two methoxy regiomers (X or Y = OCH_3). The slower eluting 1-methoxy substituted diastereomer on reverse phase HPLC chromatography, in general, appeared to be the more active of the two diastereomers, exemplified when comparing **23a/b**, **25a/b**, and **27a/b**. Each of the diastereomers, **24a/24b**, **26a/26b**, and **28a/28b**, with 3-methoxy substitution appeared comparable in terms of ALK enzyme and cellular

dx.doi.org/10.1021/jm201550q | *J. Med. Chem.* 2012, 55, 4580–4593

potency (within 3-fold). All four analogues possessing the flexible methoxyethylamino A-ring moiety displayed comparable enzyme and cellular potency, regardless of the position of the methoxy substituent. However, the isomers **25b** and **27b**, possessing the more space constrained morpholino and methylpiperazinyl fragments, were 5- to 10-fold more potent ALK enzyme inhibitors compared to their match diasteriomers, **25a** and **27a**. This translated into increase cellular activity with **25b** and **27b** being the most potent in the Karpas-299 cell assay. Another striking difference observed between methoxy substituted analogues matched pairs was the difference in ALK selectivity over IR (expressed as IR/ALK enzyme IC_{50} ratio). The 1-methoxy substituted analogues had higher IR/ALK IC_{50} ratios compared to the ratios observed with the corresponding 3-methoxy substituted analogues. Of all of the compounds evaluated, **25b** displayed the highest IR/ALK enzyme IC_{50} ratio of 662, a 15-fold improvement over **3**. As a result, this compound was profiled more extensively.

To help rationalize the observed improved selectivity for the 1-methoxy substituted analogues, both **25b** and **3** were computationally modeled in the 2XB7 (ALK) and the 3EKK (IRK) X-ray structures as illustrated in Figure 3. Both analogues

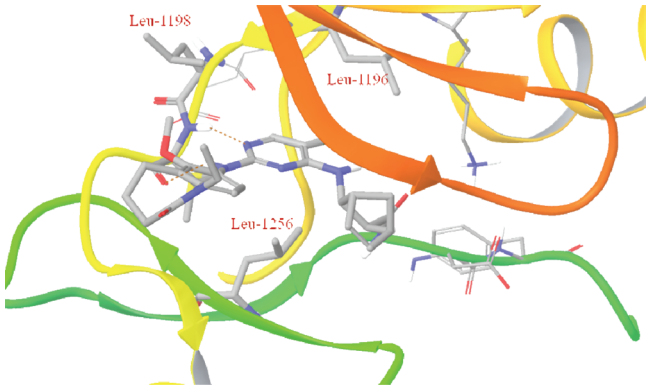

Figure 3. Binding mode of **25b** with ALK, as derived by Glide/XP docking program.

docked into the active site with the expected bidentate binding mode. This binding mode was consistent with several kinase bound 2,4-dianilinopyrimidine structures available in the Protein Data Bank.[21] Similar binding modes were also observed for IR; however, the docking scores generated computationally when modeling these structures were considerably and consistently higher (worse) for both ligands, in agreement with the observed activity. Comparison of the active site showed several critical residue differences between ALK and IR (Figure 4). The gatekeeper residue (Leu) in ALK has been replaced by Met-1076 in IR.[22] Interaction of the chloro substituent on the pyrimidine with the Leu-1196 in ALK provides a more favorable interaction compared to the more polarized Met-1076 in IR. The hydrophobic residue Leu-1256 in ALK coming from the β-sheet underneath the hinge region has been replaced by Met-1076. IR is the first kinase where the DFG-out structure was observed in the apo-form with the conformation of the activation loop differing considerably in different structures. All of these factors have affected the binding of a large ligand like **25b**, since several other IR structures failed to dock such ligands. However, the lack of activity of one of the stereoisomers of this type of ligand was resulting from the conformation difference in the loop region after the D-helix. Unlike ALK,

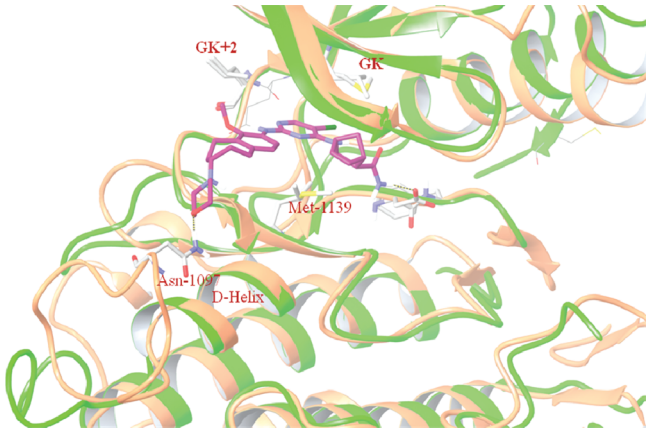

Figure 4. Binding mode of **25b** with IR (brown ribbon), as derived by Glide/XP docking program.

this loop region in IR consistently folds back toward the ATP binding pocket. With structures such as **25b**, the loop had bad steric overlap with Asn-1097 in the binding mode (Figure 4), resulting in poor IR inhibition and thus providing a possible hypothesis for the increase IR/ALK selectivity observed with **25b** compared to **3**.

Kinase selectivity for compounds in Table 1 was evaluated using Ambit's KINOMEScan panel of binding assays and expressed as an $S(90)$ value reflecting the fraction of kinases inhibited of >90% when screened at 1 μM across a panel of >353 kinases.[23] The compounds displayed in Table 1 range in $S(90)$ values from 0.03 to 0.31 with **25b** exemplifying broad kinase specificity as measured by the $S(90)$ value of 0.147. In addition, **25b** was evaluated in Millipore's KinaseProfiler panel of activity assays for 259 kinases, with IC_{50} values determined for 15 kinases inhibited by ≥90% at 1 μM (Table 2). Except for

Table 2. Millipore KinaseProfiler IC_{50} Values for 25b

kinase	IC_{50}, nM
ACK1 (h)	41 ± 6
ARK5 (h)	26 ± 3
BRK (h)	73 ± 4
CHK2 (h)	29 ± 7
FAK (h)	133 ± 15
Fer (h)	85 ± 4
Fes (h)	99 ± 36
Flt3 (h)	88 ± 4
Flt4 (h)	48 ± 11
GCK (h)	60 ± 9
JNK1a1 (h)	112 ± 17
Rsk1 (h)	61 ± 10
Rsk2 (h)	13 ± 4
Rsk3 (h)	7 ± 1
Rsk4 (h)	19 ± 11

Rsk2, -3, and -4 (IC_{50} values range of 7−19 nM), the IC_{50} for any other kinase tested is at least 10-fold higher than that for ALK (Table 2), supporting that **25b** is a highly potent and selective ALK inhibitor. Off-target kinase activities in cells could provide a more relevant assessment of kinase selectivity of **25b**.

In order to define the absolute stereochemistry of the 7-aminosubstituted 1-methoxy-6,7,8,9-tetrahydro-5*H*-benzocycloheptene amine A-ring fragment, efforts to crystallize **25a** or **25b** were undertaken. A crystal of suitable quality was achieved

dx.doi.org/10.1021/jm201550q | J. Med. Chem. 2012, 55, 4580−4593

Table 3. Pharmacokinetic Parameters of 25b in Mice, Sprague–Dawley Rat, Beagle Dog, and Cynomolgus Monkey

	PK parameter	SCID mouse	CD-1 mouse	rat	dog	monkey
iv[a]	$t_{1/2}$ (h)	1.8	0.7	0.9 ± 0.2	2.4 ± 0.2	1.2 ± 0.05
	Cl (mL min^{-1} kg^{-1})	6	29	17 ± 2	40 ± 1	28 ± 4
	V_d (L/kg)	0.8	1.8	1.3 ± 0.2	8.2 ± 0.5	2.9 ± 0.3
	AUC (ng·h/mL)	3025	584	989 ± 127	409 ± 16	615 ± 89
po[b]	C_{max} (ng/mL)	2753	880	599 ± 3	427[c]	170 ± 51
	t_{max} (h)	1	0.25	1.3 ± 0.3	0.8	4.7 ± 1.3
	$t_{1/2}$ (h)	1.8	2.3	6.2 ± 1.6	3.3	1.2 ± 0.05
	AUC (ng·h/mL)	21381	2993	4833 ± 797	2126	954 ± 209
	F (%)	71	51	50 ± 8	52	16 ± 3

[a]1 mg/kg dose. [b]10 mg/kg dose. [c]n = 2.

Table 4. Dose Escalation Data Comparison for 3 and 25b

parameter	10 mg/kg	30 mg/kg	55 mg/kg	100 mg/kg
3				
C_{max}	925 ± 192	1360 ± 106	1450 ± 115	1553 ± 71
AUC_{0-12}, ng·h/mL	6025 ± 1608	11804 ± 875	13826 ± 1163	14011 ± 562
25b				
C_{max}	349 ± 40	1006 ± 92	2253 ± 73	3053 ± 47
AUC_{0-12}, ng·h/mL	2574 ± 243	10895 ± 1000	24110 ± 1409	38187 ± 2474

with **25a** (Supporting Information). The solution of the X-ray analysis confirmed the *R*-stereochemistry of **25a**, thus conferring *S*-stereochemistry at the morpholino carbon juncture for compound **25b**.

Compound **25b** was advanced for in vivo evaluation based on the ALK cell potency, IR selectivity, and overall kinase selectivity. The pharmacokinetic properties of **25b** were evaluated in several species as highlighted in Table 3. Differences in exposure of **25b** were observed between the two mouse strains SCID and CD-1, with lower clearance and volume of distribution terms and higher AUC obtained in SCID compared to CD-1 mice. Oral exposure was demonstrated in all species with bioavailability F ranging from 16% in cynomolgus monkeys to 71% in SCID mouse.

Compound **25b** was evaluated in an oral dose escalation study in rat at 10, 30, 55, and 100 mg/kg and is summarized in Table 4. Dose proportional increases in both AUC and C_{max} were observed with **25b**, displaying a ∼9-fold increase in C_{max} and ∼15-fold increase in AUC when comparing the 10 and 100 mg/kg doses. This is in contrast to the C_{max} and AUC data for **3** at 10 and 100 mg/kg, where there is only ∼2-fold increase in C_{max} and AUC despite the 10-fold increase in dose. This comparative data between compounds **25b** and **3** highlight the improved PK exposure observed for **25b**. Efforts to advance **3** preclinically were terminated and refocused on **25b**.

A single oral dose of **25b** at 30 mg/kg led to >90% inhibition of NPM-ALK phosphorylation extending to 12 h postadministration in NPM-ALK positive ALCL Karpas-299 tumor xenograft in SCID mouse (Figure 5A). The degree of NPM-ALK phosphorylation inhibition was consistent with **25b** levels in tumor xenografts based on the calculated cellular activity of **25b** in murine plasma, suggesting that the target inhibition in tumor xenografts was likely due to direct inhibitory effects exerted by **25b** (Figure 5B).

A secondary in vivo study was measurement of the antitumor efficacy of **25b**, as assessed in a Karpas-299 tumor xenograft model in SCID mouse. Compound **25b** was administered to SCID mice orally in PEG400 at doses of 10 and 30 mg/kg b.i.d. for the 12-day duration of the study. Dose-dependent antitumor

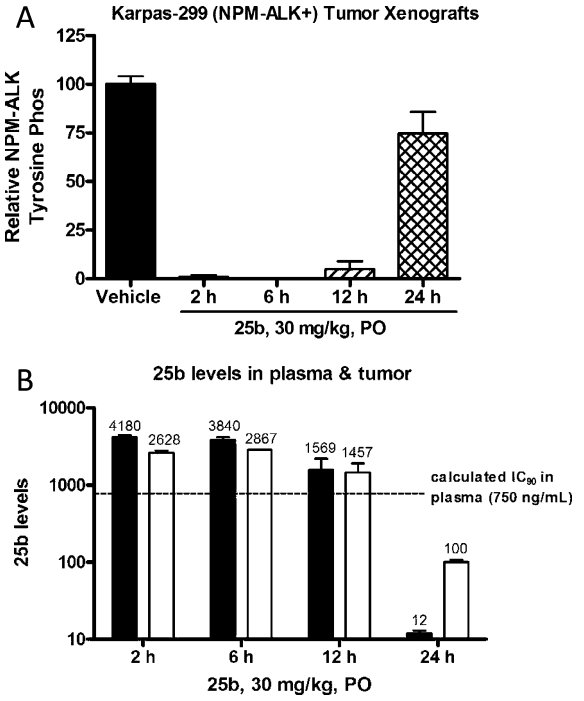

Figure 5. Pharmacodynamics of **25b** in Karpas-299 tumor xenografts in mice.

activity was observed at both oral doses of 10 and 30 mg/kg, b.i.d., with essentially complete tumor regressions achieved at the 30 mg/kg oral b.i.d. dose (Figure 6A). This is a significant improvement over **3**, which only induced tumor stasis of Karpas-299 tumor xenografts when dosed up to 100 mg/kg, b.i.d. (Supporting Information S3), consistent with the limited dose-escalation of **3** observed in rat. Administration of **25b** was well tolerated with no overt toxicity and no significant body weight loss at both dosing regimens. Dose-related levels of **25b** were observed in plasma and tumor lysates collected at 2 h after final dosing. Observed levels of **25b** in tumors were slightly less at the 10 mg/kg dose and 7-fold higher at the 30 mg/kg dose over the

dx.doi.org/10.1021/jm201550q | J. Med. Chem. 2012, 55, 4580–4593

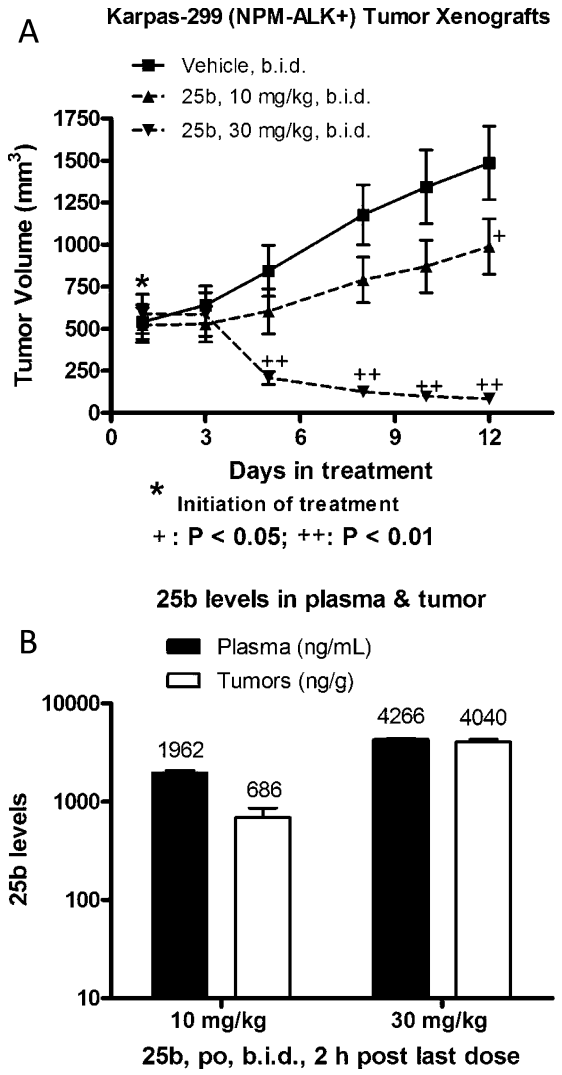

Figure 6. Antitumor efficacy of **25b** on Karpas-299 tumor xenografts in mice.

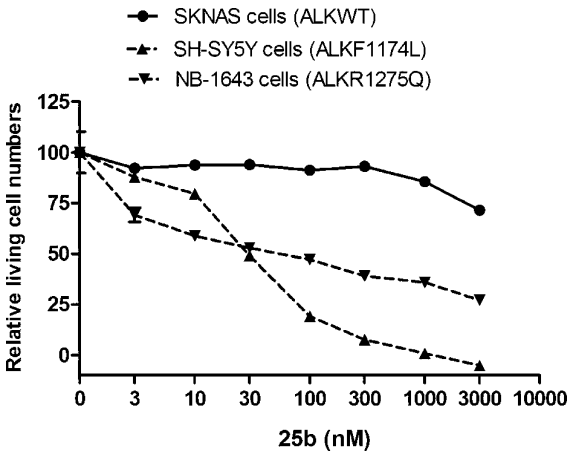

Figure 7. Growth inhibition of **25b** on neuroblastoma cell lines harboring ALK activating mutations.

plasma adjusted ALK cell IC_{90} of 1500 nM (~750 ng/mL), as measured in the presence of murine plasma (Figure 6B), further supporting the notion that sustained complete target inhibition in tumor is required to achieve regression in NPM-ALK-positive ALCL tumor xenografts.

Dose-dependent antitumor activity was also observed in other NPM-ALK-positive ALCL tumor xenografts and EML4-ALK-positive NSCLC tumor xenografts in mice administered with **25b** orally, showing complete/near complete tumor regressions following treatment at doses of 30 mg/kg b.i.d. or higher.[24] In addition, **25b** induced growth inhibition and cytotoxicity of neuroblastoma cell lines harboring ALK activating mutants (F1174L in NB-1643 cells and R1275Q in SH-SY5Y cells, respectively) but not in the ones containing ALK WT without gene amplification (SKNAS cells) (Figure 7), indicating that **25b** is active against the two ALK activating mutants most commonly observed in human neuroblastoma.

■ CONCLUSION

Optimization of the diaminopyrimidine chemotype has resulted in the identification of a potent, selective, and orally bioavailable ALK inhibitor, **25b**. This diaminopyrimidine analogue possessed marked improved selectivity versus IR compared to compound **3**. Further optimization of the diaminopyrimidine core by fixing the C-ring as the [2.2.1] fragment and re-optimizing the A-ring fragment from an azepinone ring to a substituted aminobenzocycloheptene ring has led to substantial improvements in IR/ALK selectivity over those observed for **3** and improved hERG inhibition versus **4** (Supporting Information). Molecular modeling suggests that the improvement in IR/ALK selectivity observed for **25b** may be due to unfavorable interactions with the Met1139 located underneath the hinge region. In addition to improved IR/ALK selectivity, **25b** displayed dose proportional increases in rat exposure, providing a clear advantage over compound **3**. Therefore, further preclinical development of **3** was discontinued in favor of **25b**.

Additional studies analyzing the impact of **25b** and other potent, selective, and orally bioavailable ALK inhibitors with newly identified mutants will be necessary to provide improved ALK inhibitors to treat NSCLC.[25] Compound **25b** demonstrated potent inhibitory activity against ALK phosphorylation both in vitro and in vivo and robust antitumor efficacy (tumor regressions) in Karpas-299 tumor xenografts in mice. Combining with its overall favorable pharmaceutical properties, **25b** was identified as a preclinical development candidate and was further examined in additional biological and pharmaceutical assessments. Efficacy results from more advanced preclinical models will be presented in subsequent publications.

■ EXPERIMENTAL SECTION

Chemistry. All reagents and anhydrous solvents were obtained from commercial sources and used as received. ^{1}H and ^{13}C NMR were obtained on a Bruker 400 MHz instrument in the solvent indicated with tetramethylsilane as an internal standard. Coupling constants (J) are in hertz (Hz). Analytical HPLC was run using a Zorbax RX-C8, 5 mm × 150 mm column, eluting with a mixture of acetonitrile and water containing 0.1% trifluoroacetic acid with a gradient of 10−100% over 6 min, monitoring at wavelengths 254, 290, and 215 nm. LCMS analysis was either performed on a Waters Aquity Ultra Performance LC with a 2.1 mm × 50 mm Waters Aquity UPLC BEH C18 1.7 μm column or Agilent 1100 with a 2.1 mm × 30 mm 3.5 μm Eclipse XDB-C8 column and a solvent system of 10−100% acetonitrile−water with 0.1% formic acid. The mass spectrometry data were acquired on a Micromass LC-ZQ 2000 quadrapole mass spectrometer (Waters Aquity) or a Bruker Esquire 200 ion trap (Agilent 1100) instrument. High resolution mass spectrometry was performed on a Waters Synapt G2 Q-TOF mass spectrometer by positive ion electrospray using leucine¬enkephalin as a lock-mass standard. Column chromatography was typically performed using automation on an ISCO CombiFlash

dx.doi.org/10.1021/jm201550q | J. Med. Chem. 2012, 55, 4580−4593

Companion using silica gel. Additional purification was accomplished using a Gilson preparative HPLC system and reverse phase silica gel and trilution LC software. Melting points were taken on a Mel-Temp apparatus and are uncorrected. Purity of described compounds was assessed by HPLC and shown to be >95% pure unless otherwise noted.

Preparation of 1,2-Bis-bromomethyl-3-methoxybenzene (6).[26] 1-Methoxy-2,3-dimethyl-benzene (40 g, 0.29 mol), *N*-bromosuccinimide (104.6 g, 0.5877 mol), and 2,2′-azo-bis-isobutyronitrile (2 g, 0.01 mol) were dissolved in carbon tetrachloride (800 mL). The mixture was heated to reflux and was allowed to stir overnight. The reaction mixture was cooled, and the solids were collected by filtration. The filtrate was then washed with saturated sodium bicarbonate and extracted with dichloromethane. Combined organic layers were dried over sodium sulfate, filtered, and concentrated under vacuum to give the desired product (86 g, 99% yield). ^{1}H NMR ($CDCl_3$) δ 7.23 (t, 1H, J = 8.05 Hz), 6.96 (d, 1H, J = 7.64 Hz), 6.86 (d, 1 H, J = 8.36 Hz), 4.77 (s, 2H), 4.61 (s, 2H), 3.89 (s, 3H).

Preparation of 1-Methoxy-5,6,8,9-tetrahydrobenzocyclohepten-7-one (8).[27] (i) To a 5 L flask was added tetra-*n*-butylammonium iodide (30 g, 0.09 mol) in 0.6 M of sodium bicarbonate in water (1250 mL) and methylene chloride (500 mL). The reaction mixture was cooled to 0 °C, and a solution of 1,2-bis-bromomethyl-3-methoxybenzene (43.0 g, 0.146 mol) and 3-oxopentanedioic acid, diethyl ester (34.6 mL, 0.190 mol) in methylene chloride (120 mL) was added slowly dropwise to the reaction mixture via addition funnel. Following complete addition, the reaction mixture was vigorously stirred at room temperature overnight. The mixture was transferred in batches to a separatory funnel where the layers were separated. The aqueous layer was washed with additional methylene chloride, and the combined organic extracts were dried over magnesium sulfate, filtered, and concentrated under vacuum to a dark oil. The oil was triturated with diethyl ether, and the tetrabutylammonium salts precipitated out of solution and were collected by filtration. The filtrate was concentrated under vacuum to a dark oil which was carried directly on to the next step without purification.

(ii) A stirred solution of 1-methoxy-7-oxo-6,7,8,9-tetrahydro-5*H*-benzocycloheptene-6,8-dicarboxylic acid diethyl ester (80 g, 0.2 mol) in ethanol (1500 mL, 26 mol) and aqueous potassium hydroxide solution (1 M, 950 mL) was heated to reflux for 3 h. After 3 h, the mixture was cooled to room temperature and carefully quenched with 1 N HCl. The reaction mixture was concentrated under vacuum to remove ethanol and then extracted with methylene chloride. The organic layer was dried over magnesium sulfate, filtered, and concentrated under vacuum to provide a dark brown-black oil. Purification was accomplished using ISCO chromatography on silica gel with hexane–ethyl acetate as the eluant. Fractions corresponding to product were combined and concentrated under vacuum, during which time product crystallized as a yellow solid. ^{1}H NMR ($CDCl_3$) δ 7.16 (t, 1H, J = 7.58 Hz), 6.83 (dd, 2H), 3.83 (s, 3H), 3.01 (m, 2H), 2.91 (m, 2H), 2.59 (m, 4H).

Preparation of 1-Methoxy-2-nitro-5,6,8,9-tetrahydrobenzocyclohepten-7-one (10). A flask containing 1-methoxy-5,6,8,9-tetrahydrobenzocyclohepten-7-one (5.76 g, 30.3 mmol) in acetonitrile (142.3 mL) was cooled to 0 °C, and the mixture was stirred for 5 min. Potassium nitrate (3.06 g, 30.3 mmol) was added in one portion, and the mixture was stirred for 5–10 min at 0 °C and then warmed to room temperature. Changes in color from light yellow to a deeper orange were observed over 2 h at room temperature. After 2 h, the reaction mixture was poured into saturated sodium bicarbonate. Solid bicarbonate was also added to adjust the pH between 4.5 and 6.0. The reaction mixture was extracted with methylene chloride (3 × 100 mL). The organic extracts were combined and dried over magnesium sulfate, filtered, and concentrated under vacuum to give the product as an orange waxy solid (7.55 g). Purification was accomplished on silica gel using ISCO chromatography and ethyl acetate–hexanes (0–50%) as the eluant (2.10 g, 29.5%). Additional material was isolated by subjecting the filtrate to chromatography. ^{1}H NMR ($CDCl_3$) δ 7.71 (d, 1H, J = 7.92 Hz), 7.11 (d, 1H, J = 8.29 Hz), 3.90 (s, 3H), 3.05 (m, 2H), 2.99 (m, 2H), 2.63 (m, 4H).

Preparation of 1-Bromo-2,3-bis-bromomethyl-4-methoxybenzene (7).[28] To a stirred solution of 1-methoxy-2,3-dimethylbenzene (**1**) (10.00 g, 0.073 mol) in carbon tetrachloride (100 mL, 1 mol) was added *N*-bromosuccinimide (39.2 g, 0.22 mol) and benzoyl peroxide (0.2 g, 0.7 mmol). The reaction mixture was heated to reflux overnight. Additional NBS (1 equiv) and benzoyl peroxide (0.1 equiv) were added, and the mixture continued to be heated at reflux. The reaction mixture was cooled to room temperature and succinimide removed by filtration. The filtrate was concentrated under vacuum to give product. ^{1}H NMR (DMSO-d_6) δ 7.66 (d, 1H, J = 8.84 Hz), 1.06 (d, 1H, J = 8.84 Hz), 4.81 (s, 2H), 4.77 (s, 2H), 3.88 (s, 3H).

Preparation of 1-Bromo-4-methoxy-5,6,8,9-tetrahydrobenzocyclohepten-7-one (9). (i)To a stirred suspension of tetra-*n*-butylammonium iodide (1.2 g, 0.0032 mol) in 0.6 M of sodium bicarbonate in water (43 mL) and methylene chloride (5 mL, 0.08 mol) was added a solution of 3-oxopentanedioic acid, diethyl ester (1.3 mL, 0.0070 mol) and 1-bromo-2,3-bis-bromomethyl-4-methoxybenzene (2.01 g, 0.00539 mol) in methylene chloride (5 mL) dropwise. The biphasic reaction mixture was stirred vigorously overnight, during which time the mixture changed color from pale yellow to orange. The reaction mixture was quenched with ammonium chloride and extracted with methylene chloride (3 × 30 mL). The organic extracts were dried over magnesium sulfate, filtered, and concentrated under vacuum. The diastereomeric mixture was taken on without purification to the next step.

(ii) A stirred solution of 1-bromo-4-methoxy-7-oxo-6,7,8,9-tetrahydro-5*H*-benzocycloheptene-6,8-dicarboxylic acid diethyl ester (102 g, 0.247 mol) in ethanol (2000 mL) and 1 M aqueous potassium hydroxide (1300 mL) was heated to reflux for 2 h. The reaction mixture was cooled to room temperature. HCl (1 N) was added to quench the reaction and the product extracted with methylene chloride, washed with water and brine, dried over magnesium sulfate, filtered, and concentrated under vacuum to give a light orange-tan solid. The material was purified by ISCO chromatography using ethyl acetate–hexane (25–50%) to give the desired product as a pale orange-tan solid (58 g, 87% yield). ^{1}H NMR ($CDCl_3$) δ 7.44 (d, 1H, J = 8.84 Hz), 6.70 (d, 1H, J = 9.09 Hz), 3.82 (s, 3H), 3.18 (m, 2H), 3.08 (m, 2H), 2.57 (m, 4H).

Preparation of 4-Bromo-1-methoxy-2-nitro-5,6,8,9-tetrahydrobenzocyclohepten-7-one (11). To a stirred solution of 1-bromo-4-methoxy-5,6,8,9-tetrahydrobenzocyclohepten-7-one (20.0 g, 0.074 mol) in sulfuric acid (200 mL) at 0 °C under an atmosphere of nitrogen was added potassium nitrate (7.89 g, 0.078 mol) in portions. After being stirred for 15 min, the reaction mixture was poured over ice–water. A gummy solid formed which was dissolved in methylene chloride, transferred to a separatory funnel and the water layer removed. The organic phase was washed with saturated aqueous bicarbonate and water, dried over magnesium sulfate, filtered, and concentrated under vacuum to an orange solid. Product was purified by ISCO chromatography on silica gel (350 g column) using ethyl acetate–hexane (10–100%). Fractions corresponding to product were combined and concentrated under vacuum to give product as an orange solid (18 g, 77% yield). ^{1}H NMR ($CDCl_3$) δ 8.04 (s, 1H), 3.90 (s, 3H), 3.25 (m, 2H), 3.15 (m, 2H), 2.64 (m, 4H).

Preparation of ((4-Bromo-1-methoxy-2-nitro-6,7,8,9-tetrahydro-5*H*-benzocyclohepten-7-yl)-(2-methoxyethyl)amine (13a). To a stirred solution of 4-bromo-1-methoxy-2-nitro-5,6,8,9-tetrahydrobenzocyclohepten-7-one (2.2 g, 7 mmol) in methylene chloride (150 mL) was added 2-methoxyethylamine (6.1 mL, 70.4 mmol), powdered 4 Å molecular sieves, and acetic acid (4 mL, 70.4 mmol). The reaction mixture was heated to reflux overnight and then cooled to room temperature. Sodium triacetoxyborohydride (4.5 g, 21 mmol) was added in one portion, and the mixture was stirred for 2 h. The reaction solids were removed by filtration, and the filtrate was neutralized with 33% aqueous sodium hydroxide, adjusting the pH between 8 and 10. The product was extracted with methylene chloride (3 × 30 mL). The organic extract was dried over magnesium sulfate, filtered, and concentrated under vacuum. Purification was accomplished on silica gel using methanol–methylene chloride (10%) as the eluant to give the product as a red oil. ^{1}H NMR ($CDCl_3$)

dx.doi.org/10.1021/jm201550q | J. Med. Chem. 2012, 55, 4580–4593

δ 7.93 (s, 1H), 3.85 (s, 3H), 3.51 (t, 2H, J = 6.3 Hz), 3.39 (m, 2H), 3.37 (s, 3H), 2.83 (m, 4H), 2.62 (t, 1H, J = 12 Hz), 2.08 (m, 2H), 1.33 (m, 2H).

Preparation of 4-(4-Bromo-1-methoxy-2-nitro-6,7,8,9-tetrahydro-5*H*-benzocyclohepten-7-yl)morpholine (13b). The product was isolated as a brown oil (17.8 g, 79% yield). ^{1}H NMR ($CDCl_3$) δ 7.92 (s, 1H), 3.86 (s, 3H), 3.70 (t, 4H, J = 4.5 Hz), 3.43 (m, 1H), 2.90 (t, 2H, J = 4.5 Hz), 2.68 (m, 2H), 2.55 (t, 2H, J = 4.5 Hz), 2.47 (m, 2H), 2.13 (m, 2H), 1.42 (q, 2H, J = 10 Hz).

Preparation of 1-(4-Bromo-1-methoxy-2-nitro-6,7,8,9-tetrahydro-5*H*-benzocyclohepten-7-yl)-4-methylpiperazine (13c). The product was isolated as a brown oil (1.87 g, 72% yield). ^{1}H NMR ($CDCl_3$) δ 7.96 (s, 1H), 3.96 (s, 3H), 3.72 (t, 4H, J = 4.5 Hz), 3.43 (m, 1H), 2.90 (t, 2H, J = 4.5 Hz), 2.68 (m, 2H), 2.55 (m, 2H), 2.47 (m, 2H), 2.26 (s, 3H), 2.06 (m, 2H), 1.74 (m, 2H).

Preparation of (2-Methoxyethyl)-(2-nitro-6,7,8,9-tetrahydro-5*H*-benzocyclohepten-7-yl)amine (14a). 4-Bromo-1-methoxy-2-nitro-6,7,8,9-tetrahydro-5*H*-benzocyclohepten-7-yl)-(2-methoxyethyl)amine (2.4 g, 6.4 mmol) was dissolved in ethanol (50 mL) in a 500 mL Parr flask. Palladium on carbon, 10% (90:10 carbon black/palladium, 250 mg, 19 mmol), was added to the flask and the material subjected to hydrogen at 50 psi for 16 h. The catalyst was removed by filtration through Celite and the resulting filtrate concentrated under vacuum to provide the desired product as a red oil (HBr salt). ^{1}H NMR ($CDCl_3$) δ 6.68 (d, 1H, J = 8.1 Hz), 6.52 (d, 1H, J = 8.1 Hz), 3.77 (m, 4H), 3.68 (s, 3H), 3.40 (s, 3H), 3.07 (m, 4H), 2.75 (m, 1H), 2.39 (m, 2H), 1.55 (m, 2H).

Preparation of 1-Methoxy-7-morpholin-4-yl-6,7,8,9-tetrahydro-5*H*-benzocyclohepten-2-ylamine (14b). The product was isolated as an HBr salt (11 g, 79% yield). ^{1}H NMR ($CDCl_3$) δ 6.72 (d, 1H, J = 7.83 Hz), 6.55 (d, 1H, J = 7.83 Hz), 4.15 (broad s, 4H), 3.70 (s, 3H), 3.47 (m, 1H), 3.35 (broad s, 1H), 3.10 (broad s, 4H), 2.59–2.86 (m, 4H), 2.37 (m, 1H), 1.48 (m, 3H).

Preparation of 1-Methoxy-7-(4-methylpiperazin-1-yl)-6,7,8,9-tetrahydro-5*H*-benzocyclohepten-2-ylamine (14c). The product was isolated as a dark brown oil HBr salt (1.5 g, 89%). ^{1}H NMR ($CDCl_3$) δ 6.91 (d, 1H, J = 8.84 Hz), 6.49 (s, 1H), 6.44 (d, 1H, J = 8.84 Hz), 3.63 (m, 1H), 2.54–2.75 (m, 6H), 2.31–2.45 (m, 5H), 2.31 (s, 3H), 2.05 (m, 2H), 1.61 (m, 1H), 1.37 (m, 2H).

Preparation of 1,2-Bis-bromomethyl-4-methoxybenzene (16).[29] (i) To a stirred suspension of lithium tetrahydroaluminate (16.6 g, 0.44 mol) in tetrahydrofuran (300 mL) at 0 °C under nitrogen was added dropwise a solution of 4-methoxyphthalic acid dimethyl ester (24.46 g, 0.11 mol) in tetrahydrofuran (100 mL). The mixture was stirred at 0 °C for 1 h and then warmed to room temperature overnight. The mixture was recooled at 0 °C and the reaction quenched with addition of water (125 mL) carefully dropwise, followed by 1 N NaOH (100 mL) and additional water (125 mL). Evolution of gas was observed upon initial quenching with water. Aluminum salts precipitated out of solution and were removed by filtration following complete quenching of the reaction mixture. The filtrate was diluted with ethyl acetate, washed with water, dried over magnesium sulfate, filtered, and concentrated under vacuum to provide (2-hydroxymethyl-4-methoxyphenyl)methanol as a colorless oil (17.8 g, 97% yield). ^{1}H NMR ($CDCl_3$) δ 7.24 (d, 1H, J = 8.2 Hz), 6.91 (s, 1H), 6.80 (d, 1H, J = 8.2 Hz), 4.63 (d, 4H, J = 6.3 Hz), 3.8 (s, 3H), 3.44 (broad s, 1H), 3.16 (broad s, 1H).

(ii) (2-Hydroxymethyl-4-methoxyphenyl)methanol (17.8 g, 0.11 mol) was dissolved in chloroform (200 mL, 2 mol) and treated with phosphorus tribromide (60.2 g, 0.222 mol) dropwise over 6 h. After being stirred overnight at room temperature, the mixture was cooled at 0 °C and treated with water (50 mL). The reaction mixture was poured over saturated sodium bicarbonate and extracted with dichloromethane. Combined organics were dried over sodium sulfate, filtered, and concentrated under vacuum to give the product (16.0 g, 51% yield) which was used without further purification. ^{1}H NMR ($CDCl_3$) δ 7.29 (d, 1H, J = 8.4 Hz), 6.9 (s, 1H), 6.83 (d, 1H, J = 8.4 Hz), 4.66 (s, 2H), 4.62 (s, 2H), 3.82 (s, 3H).

Preparation of 2-Methoxy-5,6,8,9-tetrahydrobenzocyclohepten-7-one (17). (i) To a stirred solution of tetra-*n*-butylammonium iodide (12.1 g, 0.033 mol) in 0.6 M of sodium bicarbonate in water (300 mL) and methylene chloride (130 mL, 2.1 mol) was added a solution of 1,2-bis-bromomethyl-4-methoxybenzene (16.00 g, 0.054 mol) and 3-oxopentanedioic acid, diethyl ester (14.31 g, 0.071 mol) in methylene chloride (40 mL, 0.6 mol). The solution was stirred vigorously at room temperature for ~20 h. Saturated ammonium chloride solution was added to the reaction mixture. The product was extracted with ethyl acetate (3 × 100 mL). The ethyl acetate extracts were washed with water and brine, then dried over magnesium sulfate, filtered, and concentrated under vacuum to give a yellow oil. The oil was triturated with ether, and a solid precipitated out of solution and was removed by filtration (tetrabutylammonium salts). The filtrate was concentrated to an oil (20.0 g, 100%) that was carried on to the next step without purification.

(ii) 2-Methoxy-7-oxo-6,7,8,9-tetrahydro-5*H*-benzocycloheptene-6,8-dicarboxylic acid diethyl ester (18.2 g, 0.0544 mol) was dissolved in ethanol, and the solution was treated with potassium hydroxide (24.4 g, 0.435 mol) in water (140 g, 7.6 mol). The mixture was then refluxed until HPLC showed consumption of starting material (~5 h). The mixture was then acidified with 1 N HCl, and the product was extracted with dichloromethane. Organic extracts were dried over sodium sulfate, filtered, and concentrated under vacuum. The crude mixture was filtered through a plug of silica, rinsing with dichloromethane before purification. The filtrate was concentrated under vacuum and purified by ISCO flash column chromatography (hexane–ethyl acetate). Combined fractions were reduced under vacuum to afford 2-methoxy-5,6,8,9-tetrahydrobenzocyclohepten-7-one (6.0 g, 58% yield). ^{1}H NMR ($CDCl_3$) δ 7.14 (d, 1H, J = 8.8 Hz), 6.79 (s, 1H), 6.75 (d, 1H, J = 8.8 Hz), 3.81 (s, 3H), 2.86 (m, 4H), 2.56 (m, 4H).

Preparation of 2-Methoxy-1-nitro-5,6,8,9-tetrahydrobenzocyclohepten-7-one (18) and 2-Methoxy-3-nitro-5,6,8,9-tetrahydrobenzocyclohepten-7-one (19). 2-Methoxy-5,6,8,9-tetrahydrobenzocyclohepten-7-one (6.00 g, 0.0315 mol) was dissolved in acetonitrile (280 mL) and was added to a mixture of trifluoroacetic anhydride (13.4 mL, 0.095 mol) in acetonitrile (60 mL) at 0 °C. Potassium nitrate (3.19 g, 0.032 mol) was then added and the mixture allowed to warm to room temperature. Following complete consumption of starting material, the mixture was poured over saturated sodium bicarbonate, and organics were extracted with ethyl acetate–dichloromethane. Combined organics were dried over sodium sulfate, filtered, and reduced under vacuum. The crude mixture was purified by ISCO flash column chromatography using hexane–ethyl acetate (0–50%). Combined fractions were reduced under vacuum to afford 2-methoxy-1-nitro-5,6,8,9-tetrahydrobenzocyclohepten-7-one (1.80 g, 25% yield) (^{1}H NMR ($CDCl_3$) δ 7.30 (d, 1H, J = 8.6 Hz), 6.90 (d, 1H, J = 8.6 Hz), 3.89 (s, 3H), 2.93 (m, 2H), 2.77 (m, 2H), 2.60–2.65 (m, 4H)) and 3.62 g (49%) of 2-methoxy-3-nitro-5,6,8,9-tetrahydrobenzocyclohepten-7-one (^{1}H NMR ($CDCl_3$) δ 7.78 (s, 1H), 6.96 (s, 1H), 3.97 (s, 3H), 2.94 (m, 4H), 2.64 (m, 4H)).

Preparation of 3-Methoxy-*N7*-(2-methoxyethyl)-6,7,8,9-tetrahydro-5*H*-benzocycloheptene-2,7-diamine (20a).** (i) To a stirred solution of 2-methoxy-3-nitro-5,6,8,9-tetrahydrobenzocyclohepten-7-one (0.81 g, 0.0034 mol) in 1,2-dichloroethane (12 mL) under nitrogen at room temperature were added 2-methoxyethylamine (0,31 g, 0.004 mol) and acetic acid (0.24 mL, 0.004 mol). The reaction mixture was stirred at room temperature for 3 h. The mixture was then cooled to 0 °C, and sodium triacetoxyborohydride (2.2 g, 0.01 mol) was added to the reaction mixture in one portion. The reaction mixture was stirred at 0 °C for 30 min and then warmed to room temperature for 4 h. The reaction mixture was quenched with water and pH adjusted to 8–10 with 10 N NaOH solution. The mixture was extracted with methylene chloride, dried over magnesium sulfate, and concentrated under vacuum. Purification was accomplished on silica gel using ISCO chromatography with methylene chloride–methanol with ammonium hydroxide. The product was isolated as a brown film. ^{1}H NMR ($CDCl_3$) δ 8.42 (s, 1H), 8.16 (s, 1H), 3.87 (s, 3H), 3.67 (m, 2H), 3.38 (m, 5H), 3.22 (m, 2H), 2.62–2.88 (m, 5H), 2.36 (m, 2H).

(ii) 2-Methoxyethyl-(2-methoxy-3-nitro-6,7,8,9-tetrahydro-5*H*-benzocyclohepten-7-yl)amine (2.50 g, 0.0085 mol) in ethanol (45 mL) was added to a Parr vessel containing palladium on carbon, 10% (90:10 carbon black/palladium, 0.5 g, 0.038 mol), under nitrogen. The

dx.doi.org/10.1021/jm201550q | J. Med. Chem. 2012, 55, 4580–4593

vessel was placed on a Parr shaker and subjected to hydrogen at 50 psi for 2 h. Catalyst was removed by filtration and the product used without purification. ^{1}H NMR ($CDCl_3$) δ 7.67 (s, 1H), 6.83 (s, 1H), 3.94 (s, 3H), 3.53 (t, 1H, J = 14 Hz), 3.37 (s, 6H), 2.83−2.92 (m, 5H), 2.71 (m, 2H), 2.12 (m, 2H), 1.39 (m, 2H).

Preparation of 3-Methoxy-7-morpholin-4-yl-6,7,8,9-tetrahydro-5*H*-benzocyclohepten-2-ylamine (20b). (i) 2-Methoxy-3-nitro-5,6,8,9-tetrahydrobenzocyclohepten-7-one (4.94 g, 0.021 mol) in methylene chloride (100 mL) was treated with morpholine (18.30 g, 0.21 mol) followed by acetic acid (12.61 g, 0.21 mol). Powdered 4 Å molecular sieves (2 mass equiv) was added and the mixture heated to reflux for 4 h. The solution was then cooled to room temperature, and sodium triacetoxyborohydride (8.90 g, 0.042 mol) was added. The reaction mixture was poured over saturated sodium bicarbonate, and organics were extracted with ethyl acetate−dichloromethane. Combined organics were dried over sodium sulfate, filtered, and concentrated under vacuum. The crude mixture was purified by ISCO flash column chromatography (methylene chloride−methanol). Combined fractions were reduced under vacuum to afford 4-(2-methoxy-3-nitro-6,7,8,9-tetrahydro-5*H*-benzocyclohepten-7-yl)morpholine (5.4 g, 84% yield).

(ii) 4-(2-Methoxy-3-nitro-6,7,8,9-tetrahydro-5*H*-benzocyclohepten-7-yl)morpholine (5.40 g, 0.018 mol) was dissolved in ethanol (100 mL) and the reaction mixture carefully added to 10% palladium on carbon (0.75 g) under nitrogen in a Parr vessel. The mixture was then placed on a Parr shaker until uptake of hydrogen had ceased (5 h). Catalyst was removed by filtration and the filtrate concentrated under vacuum to afford 3-methoxy-7-morpholin-4-yl-6,7,8,9-tetrahydro-5*H*-benzocyclohepten-2-ylamine (4.1 g, 84% yield). ^{1}H NMR (DMSO-d_6) δ 6.56 (s, 1H), 6.40 (s, 1H), 4.39 (m, 2H), 3.17 (s, 3H), 3.53 (m, 4H), 3.34 (m, 2H), 2.62 (m, 1H), 2.44 (m, 4H), 1.91 (m, 2H), 1.24 (q, 2H, J = 12 Hz).

Preparation of 3-Methoxy-7-(4-methyl-piperazin-1-yl)-6,7,8,9-tetrahydro-5*H*-benzocyclohepten-2-ylamine (20c). (i) 2-Methoxy-3-nitro-5,6,8,9-tetrahydrobenzocyclohepten-7-one (1.5 g, 6.38 mmol) and 1-methylpiperazine (6.4 g, 63.8 mmol) were dissolved in methylene chloride (150 mL) and treated with acetic acid (3.8 g, 63.8 mmol). The mixture was then heated to reflux for 4 h. When the mixture cooled to room temperature, sodium triacetoxyborohydride (2.7 g, 12.8 mmol) was added in one portion. The reaction mixture was stirred at room temperature overnight. The reaction mixture was poured over saturated aqueous sodium bicarbonate solution and extracted with dichloromethane. The organic phase was dried over sodium sulfate, filtered, and concentrated under vacuum. The crude reaction mixture was purified on silica gel using ISCO chromatography with hexane−ethyl acetate as the eluant. Fractions corresponding to product were dried to provide the desired product which was carried on without purification.

(ii) 1-(2-Methoxy-3-nitro-6,7,8,9-tetrahydro-5*H*-benzocyclohepten-7-yl)-4-methylpiperazine (1.89 g 5.92 mmol) was dissolved in ethanol (40 mL). Palladium on carbon, 10% (90:10 carbon black/palladium, 0.5 g, 37.5 mmol), was added to the reaction mixture, and the contents were placed under hydrogen (50 psi) for 2 h. The catalyst was removed by filtration through Celite and the filtrate concentrated under vacuum to give product. ^{1}H NMR (DMSO-d_6) δ 6.56 (s, 1H), 3.7 (s, 3H), 3.48 (m, 4H), 3.34 (m, 4H), 2.6 (m, 1H), 2.45 (m, 2H), 2.27 (m, 2H), 1.91 (m, 2H), 1.24 (q, 2H, J = 12 Hz).

Preparation of (1*S*,2*S*,3*R*,4*R*)-3-(2,5-Dichloropyrimidin-4-ylamino)bicyclo[2.2.1]hept-5-ene-2-carboxylic Acid Amide (22). A mixture of (2-exo,3-exo)3-aminobicyclo[2.2.1]hept-5-ene-2-carboxamide (250 mg, 1.64 mmol), 2,4,5-trichloropyrimidine (**19**) (366 mg, 1.99 mmol), and sodium bicarbonate (280 mg, 3.33 mmol) in methanol (4 mL) and water (2 mL) was stirred at room temperature for 69 h. The mixture was diluted with water (10 mL) and extracted with ethyl acetate (2 × 25 mL). The combined organic extracts were washed successively with water and brine. After drying over magnesium sulfate, the reaction mixture was filtered and concentrated under vacuum. The product was triturated with diethyl ether, filtered, and washed with additional diethyl ether. The product (2-exo,3-exo)-3-(2,5-dichloropyrimidin-4-ylamino)bicyclo [2.2.1]hept-5-ene-2-carboxamide was isolated as a white solid (276 mg, 56% yield). ^{1}H NMR (DMSO-d_6) δ 8.61 (d, 1H, J = 7.32 Hz), 8.20 (s, 1H), 7.86 (s, 1H), 7.32 (s, 1H), 6.33 (br s, 1H), 6.30 (br s, 1H), 3.99 (m, 1H), 2.88 (s, 1H), 2.75 (s, 1H), 2.04 (d, 1H, J = 8.84 Hz), 1.40 (d, 1H, J = 8.84 Hz); LCMS (m/e) 299, 300 (M + H).

General Procedure for Coupling Reactions: Preparation of (1*S*,2*S*,3*R*,4*R*)-3-[5-Chloro-2-((*S*)-1-methoxy-7-morpholin-4-yl-6,7,8,9-tetrahydro-5*H*-benzocyclohepten-2-ylamino)-pyrimidin-4-ylamino]bicyclo[2.2.1]hept-5-ene-2-carboxylic Acid Amide (23a) and (1*S*,2*S*,3*R*,4*R*)-3-[5-Chloro-2-((*R*)-1-methoxy-7-morpholin-4-yl-6,7,8,9-tetrahydro-5*H*-benzocyclohepten-2-ylamino)pyrimidin-4-ylamino]bicyclo[2.2.1]hept-5-ene-2-carboxylic Acid Amide (23b). To a microwave vial containing methoxy-7-morphoin-4-yl-6,7,8,9-tetrahydro-5*H*-benzocyclohepten-2-ylamine (56 mg, 0.2 mmol) and (1*S*,2*S*,3*R*,4*R*)-3-(2,5-dichloropyrimidin-4-ylamino)bicycle[2.2.1]hept-5-ene-2-carboxylic acid amide (50 mg, 0.2 mmol) in isopropyl alcohol (4 mL) was added 4 M HCl in 1,4-dixoane (40 μL) dropwise. The reaction mixture was subjected to microwaves at 140 °C for 50 min. The mixture was concentrated under vacuum to remove solvent and purified by reverse phase preparative HPLC with acetonitrile−water containing 0.1% TFA (5−50% over 17 min) as the eluant. Two diastereomers were isolated, redissolved in methanol (3 mL), and treated separately with MP-carbonate (solid support). The MP-carbonate beads were removed by filtration and the respective filtrates concentrated under vacuum.

(1*S*,2*S*,3*R*,4*R*)-3-[5-Chloro-2-((*R*)-1-methoxy-7-morpholin-4-yl-6,7,8,9-tetrahydro-5*H*-benzocyclohepten-2-ylamino)-pyrimidin-4-ylamino]bicyclo[2.2.1]hept-5-ene-2-carboxylic Acid Amide (25a). The product was isolated as tan solid (35.6 mg, 33% yield). ^{1}H NMR ($CDCl_3$) δ 8.02 (d, 1H, J = 8.3 Hz), 7.81 (s, 1H), 6.88 (d, 1H, J = 8.3 Hz), 6.31 (m, 1H), 6.25 (m, 1H), 5.85 (s, 1H), 5.55 (s, 1H), 4.19 (t, 1H, J = 7.3 Hz), 3.01 (s, 4H), 3.72 (s, 3H), 3.49 (m, 2H), 3.07−3.15 (m, 4H), 2.91 (m, 2H), 2.76 (m, 1H), 2.38−2.47 (m, 3H), 2.18 (d, 1H, J = 9.6 Hz), 1.61 (d, 1H, J = 9.3 Hz), 1.48 (m, 2H). ^{13}C (NMR) δ 176.01, 157.99, 156.38, 152.82, 146.59, 139.08, 137.47, 136.43, 134.74, 130.79, 123.79, 117.48, 103.77, 66.65, 65.74, 61.01, 52.12, 48.66, 47.58, 46.95, 43.55, 43.43, 31.64, 29.53, 29.36, 22.82. LCMS (m/e) 539 (M + H). HRMS: calcd for $C_{28}H_{35}ClN_6O_3$ (M + H)$^+$ 539.2537, found 539.2542.

(1*S*,2*S*,3*R*,4*R*)-3-[5-Chloro-2-((*S*)-1-methoxy-7-morpholin-4-yl-6,7,8,9-tetrahydro-5*H*-benzocyclohepten-2-ylamino)-pyrimidin-4-ylamino]bicyclo[2.2.1]hept-5-ene-2-carboxylic Acid Amide (25b). The product was isolated as an off-white solid (42.8 mg, 39% yield). ^{1}H NMR ($CDCl_3$) δ 8.16 (d, 1H, J = 7.5 Hz), 7.86 (s, 2H), 7.41 (broad s, 1H), 6.88 (d, 1H, J = 7.5 Hz), 6.31 (s, 2H), 5.81 (s, 1H), 5.62 (s, 1H), 4.28 (m, 1H), 3.97 (s, 4H), 3.73 (s, 3H), 3.39−3.54 (m, 2H), 3.09 (m, 4H), 2.90 (m, 2H), 2.75 (m, 1H), 2.36−2.5 (m, 4H), 2.20 (d, 1H, J = 9 Hz), 1.61 (d, 1H, J = 9 Hz), 1.48 (m, 2H), 1.26 (m, 1H). ^{13}C NMR (DMSO-d_6) δ 175.99, 157.98, 156.36, 152.83, 146.71, 139.09, 137.57, 136.42, 134.80, 130.76, 123.77, 117.54, 103.72, 67.04, 66.71, 61.00, 52.09, 48.67, 47.56, 46.92, 43.53, 43.42, 31.66, 29.56, 29.43, 22.85. LCMS (m/e) 539 (M + H). HRMS: calcd for $C_{28}H_{35}ClN_6O_3$ (M + H)$^+$ 539.2537, found 539.2533.

(1*S*,2*S*,3*R*,4*R*)-3-{5-Chloro-2-[1-methoxy-7-(2-methoxy-ethyl-amino)-6,7,8,9-tetrahydro-5*H*-benzocyclohepten-2-ylamino]-pyrimidin-4-ylamino}bicyclo[2.2.1]hept-5-ene-2-carboxylic Acid Amide (23a). The product was isolated as the beige foam (58.2 mg, 27% yield). ^{1}H NMR ($CDCl_3$) δ 8.17 (d, J = 8.3 Hz, 1H), 7.88 (s, 1H), 7.39 (s, 1H), 6.94 (m, 1H), 6.86 (d, J = 8.4 Hz, 1H), 6.37 (m, 1H), 6.31 (m, 1H), 5.61 (br s, 1H), 5.36 (br s, 1H), 4.37 (m, 1H), 3.72 (s, 3H), 3.51 (m, 2H), 3.26 (s, 3H), 3.23 (m, 1H), 3.06 (s, 1H), 2.94 (s, 1H), 2.85−2.70 (m, 6H), 2.49 (d, J = 8.4 Hz, 2H), 2.24 (d, J = 8.9 Hz, 1H), 2.09 (m, 2H), 1.63 (m, 2H), 1.26 (m, 4H). ^{13}C NMR (DMSO-d_6): δ 175.99, 157.99, 156.37, 152.83, 146.62, 139.08, 137.73, 136.44, 134.94, 130.68, 123.72, 117.43, 103.71, 71.91, 60.96, 57.85, 52.09, 47.57, 46.91, 45.74, 43.54, 43.43, 34.09, 33.55, 30.74, 21.85. HPLC purity: >90%. LCMS (m/e) 527 (M + H). HRMS: calcd for $C_{27}H_{35}ClN_6O_3$ (M + H)$^+$ 527.2537, found 539.2538.

(1*S*,2*S*,3*R*,4*R*)-3-{5-Chloro-2-[1-methoxy-7-(2-methoxyethy-lamino)-6,7,8,9-tetrahydro-5*H*-benzocyclohepten-2-ylamino]-pyrimidin-4-ylamino}bicyclo[2.2.1]hept-5-ene-2-carboxylic Acid Amide (23b). The product was isolated as a beige foam (45.27 mg,

dx.doi.org/10.1021/jm201550q | J. Med. Chem. 2012, 55, 4580−4593

23% yield). ^{1}H NMR ($CDCl_3$) δ 8.17 (d, J = 8.3 Hz, 1H), 7.88 (s, 1H), 7.39 (s, 1H), 6.94 (m, 1H), 6.86 (d, J = 8.4 Hz, 1H), 6.37 (m, 1H), 6.31 (m, 1H), 5.61 (br s, 1H), 5.36 (br s, 1H), 4.37 (m, 1H), 3.72 (s, 3H), 3.51 (m, 2H), 3.26 (s, 3H), 3.23 (m, 1H), 3.06 (s, 1H), 2.94 (s, 1H), 2.85 − 2.70 (m, 6H), 2.49 (d, J = 8.4 Hz, 2H), 2.24 (d, J = 8.9 Hz, 1H), 2.09 (m, 2H), 1.63 (m, 2H), 1.26 (m, 4H). ^{13}C NMR (DMSO-d_6) δ 176.00, 157.97, 156.35, 152.83, 146.65, 139.09, 137.73, 136.43, 134.95, 130.69, 123.73, 117.4, 103.69, 71.90, 60.96, 57.85, 52.08, 47.56, 46.91, 45.74, 43.53, 43.41, 34.10, 33.57, 30.73, 28.91, 21.99. LCMS (m/e) 527 (M + H). HRMS: calcd for $C_{27}H_{35}ClN_6O_3$ $(M + H)^+$ 527.2537, found 539.2531.

(1*S*,2*S*,3*R*,4*R*)-3-{5-Chloro-2-[3-methoxy-7-(2-methoxyethylamino)-6,7,8,9-tetrahydro-5*H*-benzocyclohepten-2-ylamino]-pyrimidin-4-ylamino}bicyclo[2.2.1]hept-5-ene-2-carboxylic Acid Amide (24a). The product was isolated as a white trifluoroacetic acid salt (20.5 mg, 20% yield). ^{1}H NMR ($CDCl_3$) δ 10.63 (broad s, 1H), 9.38 (broad s, 1H), 8.99 (d, 1H, J = 8.08 Hz), 8.45 (broad s, 1H), 7.63 (s, 1H), 7.22 (s, 1H), 6.71 (s, 1H), 6.53 (s, 1H), 6.29 (s, 1H), 5.94 (s, 1H), 5.47 (s, 1H), 3.83 (s, 4H), 3.72 (m, 2H), 3.41 (s, 3H), 3.35 (m, 1H), 3.25 (m, 2H), 3.01 (s, 1H), 2.69−2.85 (m, 5H), 2.54 (d, 1H, J = 7.58 Hz), 2.38 (m, 2H), 2.06 (d, 1H, J = 9.09 Hz), 1.63 (m, 3H), 1.52 (d, 1H, J = 9.09 Hz). ^{13}C NMR (DMSO-d_6) δ 174.84, 157.80, 156.39, 152.85, 146.29, 139.19, 136.39, 136.09, 133.79, 126.06, 120.17, 111.60, 103.57, 73.78, 71.79, 59.90, 57.91, 57.85, 55.73, 51.82, 47.62, 46.72, 45.68, 43.77, 34.27, 34.00,31.05. LCMS (m/e) 527 (M + H). HRMS: calcd for $C_{27}H_{35}ClN_6O_3$ $(M + H)^+$ 527.2537, found 527.2554.

(1*S*,2*S*,3*R*,4*R*)-3-{5-Chloro-2-[3-methoxy-7-(2-methoxyethylamino)-6,7,8,9-tetrahydro-5*H*-benzocyclohepten-2-ylamino]-pyrimidin-4-ylamino}bicyclo[2.2.1]hept-5-ene-2-carboxylic Acid Amide (24b). The product was isolated as a white trifluoroacetic acid salt (18.9 mg, 18% yield). ^{1}H NMR ($CDCl_3$) δ 10.23 (broad s, 1H), 9.37 (broad s, 1H), 8.82 (s, 1H), 8.54 (s, 1H), 7.67 (s, 1H), 7.52 (s, 1H), 6.80 (s, 1H), 6.68 (s, 1H), 6.35 (s, 1H), 6.12 (s, 1H), 5.54 (s, 1H), 4.18 (m, 1H), 3.84 (s, 3H), 3.71 (m, 2H), 3.40 (m, 4H), 3.23 (m, 2H), 3.05 (s,1H), 2.63−2.83 (m, 4H), 2.36 (m, 2H), 2.17 (d, 2H, J = 8.59 Hz), 1.60 (m, 4H). ^{13}C NMR (DMSO-d_6) δ 175.83, 157.83, 156.38, 152.83, 146.41, 139.17, 136.43, 136.16, 133.77, 126.00, 120.42, 111.60, 103.60, 73.78, 71.63, 59.89, 57.85, 55.70, 51.78, 47.63, 46.69, 45.63, 43.81, 43.75, 34.00, 33.75, 30.94. LCMS (m/e) 527 (M + H). HRMS: calcd for $C_{27}H_{35}ClN_6O_3$ $(M + H)^+$ 527.2537, found 527.2536.

(1*S*,2*S*,3*R*,4*R*)-3-[5-Chloro-2-(3-methoxy-7-morpholin-4-yl-6,7,8,9-tetrahydro-5*H*-benzocyclohepten-2-ylamino)-pyrimidin-4-ylamino]bicyclo[2.2.1]hept-5-ene-2-carboxylic Acid Amide (26a). The product was isolated as an off-white powder (439 mg, 26% yield). ^{1}H NMR (DMSO-d_6) δ 9.60 (m, 1H), 8.12 (s, 1H), 7.90 (s, 1H), 7.79 (m, 1H), 7.39 (s, 1H), 6.98 (s, 1H), 6.36 (m, 1H), 6.16 (m, 1H), 4.00 (m, 3H), 3.83 (s, 3H), 3.30 (m, 5H), 2.74 − 2.90 (m, 6H), 2.39 (m, 3H), 1.94 (d, 1H, J = 4.80 Hz), 1.44 (m, 3H), 1.28 (m, 1H), 1.04 (s, 1H), 0.74 (s, 1H). ^{13}C NMR (DMS0-d_6) δ 175.84, 157.82, 156.38, 152.86, 146.39, 139.18, 136.39, 135.99, 133.67, 126.12, 120.30, 111.62, 103.57, 67.29, 66.71, 55.74, 51.80, 48.60, 47.63, 46.72, 43.76, 32.08, 32.03, 29.97, 29.66, 15.06. LCMS (m/e) 539. HRMS: calcd for $C_{28}H_{35}ClN_6O_3$ $(M + H)^+$ 539.2537, found 539.2534.

(1*S*,2*S*,3*R*,4*R*)-3-[5-Chloro-2-(3-methoxy-7-morpholin-4-yl-6,7,8,9-tetrahydro-5*H*-benzocyclohepten-2-ylamino)-pyrimidin-4-ylamino]bicyclo[2.2.1]hept-5-ene-2-carboxylic Acid Amide (26b). The product was was isolated as a single diastereomer as an off-white solid (422 mg, 25% yield). ^{1}H NMR (DMSO-d_6) δ 9.56 (m, 1H), 8.05 (s, 1H), 7.81 (m, 2H), 7.35 (s, 1H), 6.89 (s, 1H), 6.35 (m, 1H), 6.16 (m, 1H), 4.04 (m, 4H), 3.83 (s, 3H), 3.71 (m, 4H), 2.90 (m, 3H), 2.76 (m, 5H), 2.32 (m, 3H), 2.13 (m, 1H), 1.41 (m, 4H). ^{13}C NMR (DMSO-d_6) δ 175.83, 157.85, 156.39, 152.82, 146.52, 139.12, 136.46, 136.07, 133.68, 126.08, 120.54, 111.63, 103.64, 67.09, 66.71, 63.37, 55.73, 51.80, 48.66, 47.63, 46.70, 43.81, 31.94, 30.05, 29.87, 29.75. LCMS (m/e) 539. HRMS: calcd for $C_{28}H_{35}ClN_6O_3$ $(M + H)^+$ 539.2537, found 539.2560.

(1*S*,2*S*,3*R*,4*R*)-3-{5-Chloro-2-[1-methoxy-7-(4-methylpiperazin-1-yl)-6,7,8,9-tetrahydro-5*H*-benzocyclohepten-2-ylamino]-pyrimidin-4-ylamino}bicyclo[2.2.1]hept-5-ene-2-carboxylic Acid Amide (27a). The product was was isolated as an off-white solid (21.7 mg, 7% yield). ^{1}H NMR ($CDCl_3$) δ 11.74 (s, 1H), 9.13 (d, 1H, J = 8.08 Hz), 7.71 (s, 1H), 7.62 (d, 1H, J = 8.34), 6.90 (d, 1H, J = 8.34 Hz), 6.30 (m, 1H), 6.10 (m, 1H), 5.91 (s, 1H), 5.53 (s, 1H), 4.00 (t, 1H, J = 7.32 Hz), 3.72 (s, 3H), 3.42−3.58 (m, 8H), 3.08 (s, 1H), 2.90 (m, 1H), 2.88 (s, 1H), 2.83 (s, 3H), 2.75 (m, 2H), 2.35−2.45 (m, 6H), 2.10 (d, 1H, J = 10 Hz), 1.59 (d, 1H, J = 8.33 Hz), 1.49 (m, 2H). ^{13}C NMR (DMSO-d_6) δ 176.42, 156.88, 154.09, 147.86, 139.46, 138.5, 136.11, 134.46, 129.48, 124.28, 119.39, 118.2, 115.5, 104.27, 67.42, 61.46, 52.96, 51.18, 47.73, 47.56, 45.19, 43.58, 42.77, 42.33, 30.86, 27.95, 22.22. LCMS (m/e) 552 (M + H). LCMS (m/e) 539. HRMS: calcd for $C_{29}H_{38}ClN_7O_2$ $(M + H)^+$ 552.2854, found 552.2866.

(1*S*,2*S*,3*R*,4*R*)-3-{5-Chloro-2-[1-methoxy-7-(4-methylpiperazin-1-yl)-6,7,8,9-tetrahydro-5*H*-benzocyclohepten-2-ylamino]-pyrimidin-4-ylamino}bicyclo[2.2.1]hept-5-ene-2-carboxylic Acid Amide (27b). The product was was isolated as an off-white solid (12.6 mg, 4% yield). ^{1}H NMR ($CDCl_3$) δ 10.98 (s, 1H), 9.26 (d, 1H, J = 7.07 Hz), 7.68 (s, 1H), 7.43 (d, 1H, J = 8.09 Hz), 6.92 (d, 1H, J = 8.08 Hz), 6.58 (s, 1H), 6.20 (m, 1H), 5.91 (m, 1H), 5.52 (s, 1H), 3.80 (m, 1H), 3.70 (s, 3H), 3.39−3.62 (m, *H), 3.03 (s, 1H), 2.93 (m, 2H), 2.85 (s, 3H), 2.77 (m, 2H), 2.38 (m, 5H), 1.53 (d, 1H, J = 9.34 Hz), 1.45 (d, 1H, J = 12.4 Hz), 1.27 (m, 2H). LCMS (m/e) 552 (M + H). HRMS: calcd for $C_{29}H_{38}ClN_7O_2$ $(M + H)^+$ 552.2854, found 552.2866.

(1*S*,2*S*,3*R*,4*R*)-3-{5-Chloro-2-[3-methoxy-7-(4-methylpiperazin-1-yl)-6,7,8,9-tetrahydro-5*H*-benzocyclohepten-2-ylamino]-pyrimidin-4-ylamino}bicyclo[2.2.1]hept-5-ene-2-carboxylic Acid Amide (28a). The product was was isolated as a light brown powder (19.5 mg, 12% yield). ^{1}H NMR (400 MHz, DMSO-d_6) δ 8.12 (s, 1H), 7.89 (s, 1H), 7.78 (m, 1H), 7.38 (s, 1H), 6.96 (s, 1H), 6.35 (m, 1H), 6.14 (m, 1H), 4.02 (m, 2H), 3.82 (s, 3H), 3.50 (m, 4H), 3.30 (m, 3H), 3.14 (m, 2H), 2.78 (s, 3H), 2.71−2.92 (m, 6H), 2.16 (m, 2H), 2.05 (m, 2H), 1.43 (m, 4H). LCMS (m/e) 552 (M + H). HRMS: calcd for $C_{29}H_{38}ClN_7O_2$ $(M + H)^+$ 552.2854, found 552.285.

(1*S*,2*S*,3*R*,4*R*)-3-{5-Chloro-2-[3-methoxy-7-(4-methylpiperazin-1-yl)-6,7,8,9-tetrahydro-5*H*-benzocyclohepten-2-ylamino]-pyrimidin-4-ylamino}bicyclo[2.2.1]hept-5-ene-2-carboxylic Acid Amide (28b). The product was isolated as a light brown powder (23.8 mg, 14% yield). ^{1}H NMR (DMSO-d_6) δ 8.12 (s, 1H), 7.89 (s, 1H), 7.78 (m, 1H), 7.38 (s, 1H), 6.96 (s, 1H), 6.35 (m, 1H), 6.14 (m, 1H), 4.02 (m, 2H), 3.82 (s, 3H), 3.50 (m, 4H), 3.30 (m, 3H), 3.14 (m, 2H), 2.78 (s, 3H), 2.71−2.92 (m, 6H), 2.16 (m, 2H), 2.05 (m, 2H), 1.43 (m, 4H). HPLC purity: >86%. LCMS (m/e) 552 (M + H). HRMS: calcd for $C_{29}H_{38}ClN_7O_2$ $(M + H)^+$ 552.2854, found 552.2861.

Anaplastic Lymphoma Kinase (ALK) Assay. Compounds were tested for their ability to inhibit the kinase activity of baculovirus-expressed human ALK cytoplasmic domain using a modification of the assay protocol reported for trkA.[30] Phosphorylation of the substrate, phospholipase C-γ (PLC-γ) generated as a fusion protein with glutathione S-transferase (GST),[31] was detected with a europium-labeled antiphosphotyrosine antibody and measured by time-resolved fluorescence (TRF). Briefly, each 96-well plate was coated with 100 μL/well of 10 μg/mL substrate solution (recombinant GST-PLCγ) in Tris-buffered saline (TBS). The ALK assay mixture (total volume of 100 μL/well) consisting of 20 mM HEPES (pH 7.2), 1 μM ATP, 5 mM $MnCl_2$, 0.1% BSA, and test compound (diluted in DMSO, 2.5% DMSO final in assay) was then added to the assay plate. Enzyme (50 ng/mL ALK) was added, and the reaction was allowed to proceed at 37 °C for 15 min. Detection of the phosphorylated product was performed by adding 100 μL/well of Eu-N1 labeled PT66 antibody diluted 1:5000 in 0.25% BSA in TBS containing 0.1% Tween-20 (TBS-T). Incubation at 37 °C then proceeded for 1 h, followed by addition of 100 μL of enhancement solution. The plate was gently agitated, and after 30 min, the fluorescence of the resulting solution was measured using the PerkinElmer EnVision 2102 (or 2104) multilabel plate reader (PerkinElmer, Waltham, MA). Data analysis was performed using ActivityBase (IDBS, Guilford, U.K.). IC_{50} values were calculated by plotting percent inhibition versus $\log_{10}$ of the concentration of compound and fitting to the nonlinear regression sigmoidal dose−response (variable slope) equation in XLFit (IDBS, Guilford, U.K.).

Insulin Receptor (IR) Kinase Assay. The IR kinase assay was performed using the TRF assay as described above for ALK. The nucleotide substrate ATP was used at 20 μM, and recombinant human baculovirus-expressed IR cytoplasmic domain was added to the assay at a final concentration of 20 ng/mL. In place of Eu-N1 labeled PT66 antibody, Eu-N1 labeled PY100 antibody (diluted 1:10000 in antibody dilution buffer) was utilized for detection.

Cellular NPM-ALK Phosphorylation Assay. The cellular NPM-ALK tyrosine phosphorylation assay was carried out as described previously.[19] To calculate the cellular IC_{90} values in murine plasma, the Karpas-299 cells were incubated with different concentrations of CEP-28122 in murine plasma for about 2 h, and the cells were then processed for NPM-ALK phosphorylation assay as described.[20]

X-ray Crystallography. The X-ray intensity data were measured on a Bruker CCD area detector system (Cu Kα, 2631 frames, 0.5° in ω for 30 s): orthorhombic, $P2_12_12_1$, a = 5.1493(6) Å, b = 18.930(2) Å, c = 27.837(3) Å, Z = 4, $C_{28}H_{35}ClN_6O_3$. Solved and refined using SHELXTL (Bruker, version 6.1), the final anisotropic full-matrix least-squares refinement on F^2 (4110 reflections, 345 variables) converged at R1 = 9.25% for the observed data and wR2 = 24.22% for all data. The absolute stereochemistry can be assigned at a 99.5% reliability level with a Flack parameter of 0.08(5) for the stereochemistry as shown and 0.91(5) for the inverted model. The expected value is 0 for the correct absolute configuration and 1 for the inverted stereochemistry. The Hamilton R-factor ratio is 0.234/0.220 = 1.054, indicating greater than 99.5% reliability in the determination of the difference between the two models.

Pharmacokinetics. Adult female SCID mice, male CD-1 mice, male Sprague–Dawley rat (Charles River, Kingston, NY), male beagle dogs (Cephalon, Inc., Maisons Alfort, France), and male cynomolgus monkeys (Covance Laboratories, Alice, TX) were used in the experiments. All animal usage was approved by the Cephalon IACUC. Mice were dosed via the lateral tail vein for iv administration (3% DMSO, 30% Solutol, 67% phosphate buffered saline) or via oral gavage (100% PEG400) using a dose volume of 100 μL. Trunk blood was collected from three mice per time point over a 6 h period. Rats were also dosed via the lateral tail vein for iv administration (1 mL/kg, vehicle as described above) or via oral gavage (5 mL/kg in 40% HPβCD). Serial blood samples were collected from the lateral tail vein into heparinized collection tubes over a 6 h period. In dogs and primate iv administration (0.5 mL/kg in 40% HPβCD) was via the saphenous vein. Dogs received a 1 mL/kg oral dose via gavage, while monkeys were dosed via nasogastric tube (2 mL/kg). Serial blood samples were collected from the femoral vein into heparinized collection tubes over a 24 h period. All animals were fasted overnight prior to oral administration. The plasma was separated by centrifugation, and the sample was prepared for analysis by protein precipitation with acetonitrile. The plasma samples were analyzed for drug and internal standard via LCMS/MS protocol. The pharmacokinetic parameters were calculated by a noncompartmental method using WinNonlin software (Professional, version 4.1, Pharsight Corporation, Palo Alto, CA, 1997). Parameters were calculated using plasma concentration time data for individual animals (rat, dog, and monkey, n = 3), and these data are presented as the mean ± SEM. Mouse data are presented as the composite mean.

Pharmacodynamics. Scid mice bearing Karpas-299 sc tumor xenografts were administered **25b** at 30 mg/kg, po. P-NPM-ALK and total NPM-ALK in tumor samples were detected by immunoblotting, and relative NPM-ALK phosphorylation was calculated as described previously[22] and presented as the mean ± standard error of mean (SEM). The compound levels in plasma and tumor lysates were measured by LCMS/MS and presented as the mean ± standard error of mean.

Antitumor Efficacy Studies in Karpas-299 sc Tumor Xenografts in Mice. SCID/beige mice (6- to 8-week-old female) were maintained 5/cage in microisolator units on a standard laboratory diet (Teklad Labchow, Harlan Teklad, Madison, WI) and housed under humidity- and temperature-controlled conditions, and the light/dark cycle was set at 12 h intervals. Exponentially growing cells were implanted subcutaneously to the left flank of each mouse. The mice were monitored. When the tumor xenograft volumes reached approximately 600 mm^3, the tumor-bearing mice were randomized into different treatment groups (8–10 mice/group) and were administered orally with either vehicle (PEG-400) or compound **20b** formulated in vehicle at indicated doses and with indicated dosing frequency, with 100 μL per dosing volume. The length (L) and width (W) of each tumor was measured with a vernier caliper, and the mouse body weight was determined every 2–3 days. The tumor volumes were then calculated with the formula $0.5236LW(L + W)/2$. Statistical analyses of tumor volumes and mouse body weight were carried out using the Mann–Whitney rank sum test. Plasma and tumor samples were obtained at 2 h after final dose, and the compound levels in plasma and tumor lysates were measured by LCMS/MS.

Docking Study. The computational work was done using Schrodinger/Maestro molecular modeling package (Maestro, version 9.1.107, Schrodinger, LLC, New York, NY). The essential steps in the current docking experiment included preparation of representative ALK (PDB code 2XB7) and IRK (PDB code 3EKK) structures from the Protein Data Bank using Maestro protein preparation workflow. These structures had similar ligands and were expected to give the best docking results. The procedure involved (1) grid generation around the ligand, (2) preparation of ligands (**25b** and **3**) using the LigPrep module, (3) use of Glide/XP docking to keep the top 10 binding poses for each compound, and (4) selection of the binding mode using our knowledge based approach.[32]

■ ASSOCIATED CONTENT

Ⓢ Supporting Information

Structure of compound **25a**, hERG inhibition data for select inhibitors, and antitumor efficacy of compound **3**. This material is available free of charge via the Internet at http://pubs.acs.org.

■ AUTHOR INFORMATION

Corresponding Author

*E-mail: degingrich12@gmail.com.

Notes

The authors declare no competing financial interest.

■ ACKNOWLEDGMENTS

The authors gratefully acknowledge the scientific contributions of James Haley and Renee Roemmele for the preparation of key intermediates. Special thanks are given to Damaris Rolon-Steele, Kelli Zeigler, Christine LoSardo, and Rebecca Brown for their efforts with the pharmacokinetic data generation and analysis. The authors also thank Edward Hellriegel and Mehran Yazdanian for their contributions regarding the dog and monkey pharmacokinetic studies, Dr. Yael Mosse of Children Hospital of Philadelphia, PA, for kindly providing the neuroblastoma cell lines (SKNAS, SH-SY5Y, and NB-1643), and Henry Breslin for scientific discussion contributions.

■ REFERENCES

(1) *Cancer Facts and Figures 2011*; American Cancer Society: Atlanta, GA, 2011.

(2) (a) De Bono, J. S.; Ashworth, A. Translating cancer research into targeted therapeutics. *Nature* **2010**, *467*, 543–549. (b) Stegmeier, F.; Warmuth, M.; Sellers, W. R.; Dorsch, M. Targeted cancer therapies in the the twenty-first century: lessons from imatinib. *Clin. Pharm. Ther.* **2010**, *87* (5), 543–552.

(3) Baker, S. J.; Reddy, E. P. Targeted inhibition of kinases in cancer therapy. *Mt. Sinai J. Med.* **2010**, *77*, 573–586.

(4) (a) Milkiewicz, K. L.; Ott, G. R. Inhibitors of anaplastic lymphoma kinase: a patent review. *Expert Opin. Ther. Pat.* **2010**, *20* (12), 1653–1681. (b) Ardini, E.; Magnaghi, P.; Orsini, P.; Menichincheri, M. Anaplastic lymphoma kinase: role in specific

tumours, and development of small molecule inhibitors for cancer therapy. *Cancer Lett.* **2010**, *299*, 81−94.
(5) (a) Gerber, D. E.; Minna, J. D. ALK inhibition for non-small cell lung cancer: from discovery to therapy in record time. *Cancer Cell* **2010**, *18*, 548−551. (b) Goldstraw, P.; Ball, D.; Jett, J. R.; Le Chvalier, T.; Lum, E.; Nicholson, A. G.; Shepherd, F. A. Non-small-cell lung cancer. *Lancet* **2011**, *378*, 1727−1740. (c) Cheng, M.; Ott, G. R. Anaplastic lymphoma kinase as a therapeutic target in anaplastic large cell lymphoma, non-small cell lung cancer and neruoblastoma. *Anti-Cancer Agents Med. Chem.* **2010**, *10*, 236−249.
(6) Morris, S. W.; Kirstein, M. N.; Valentine, M. B.; et al. Fusion of a kinase gene, ALK, to a nucleolar protein gene, NPM, in non-Hodgkin's lymphoma. *Science* **1994**, *263*, 1281−1284.
(7) (a) Chiarle, R.; Voena, C.; Ambrogio, C.; Piva, R.; Inghirami, G. The anaplastic lymphoma kinase in the pathogenesis of cancer. *Nat. Rev. Cancer* **2008**, *8*, 11−23. (b) Webb, T. R.; Slavish, J.; George, R. E.; Look, A. T.; Xue, L.; Jiang, Q.; Cui, X.; Rentrop, W. B.; Morris, S. W. Anaplastic lymphoma kinase: role in cancer pathogenesis and small-molecule inhibitor development for therapy. *Expert Rev. Anticancer Ther.* **2009**, *9*, 331−356.
(8) Grande, E.; Bolos, M.; Arriola, E. Targeting oncogenic ALK: A promising strategy for cancer treatment. *Mol. Cancer Ther.* **2011**, *10* (4), 569−571.
(9) (a) Mossé, Y. P.; Laudenslager, M.; Longo, L.; Cole, K. A.; Wood, A.; Attiyeh, E. F.; Laquaglia, M. J.; Sennett, R.; Lynch, J. E.; Perri, P.; Laureys, G.; Speleman, F.; Kim, C.; Hou, C.; Hakonarson, H.; Torkamani, A.; Schork, M. J.; Brodeur, G. M.; Tonini, G. P.; Rappaport, E.; Devoto, M.; Maris, J. M. Identification of ALK as a major familial neuroblastoma predisposition gene. *Nature* **2008**, *455*, 930−936. (b) Janoueix-Lerosey, I.; Lequin, D.; Brugières, L.; Ribeiro, A.; de Pontual, L.; Combaret, V.; Raynal, V.; Puisieux, A.; Schleiermacher, G.; Pierron, G.; Valteau-Couanet, D.; Frebourg, T.; Michon, J.; Lyonnet, S.; Amiel, J.; Delattre, O. Somatic and germline activating mutations of the ALK kinase receptor in neuroblastoma. *Nature* **2008**, *455*, 967−970. (c) Chen, Y.; Takita, J.; Choi, Y. L.; Kato, M.; Ohira, M.; Sanada, M.; Wang, L.; Soda, M.; Kikuchi, A.; Igarashi, T.; Nakagawara, A.; Hayashi, Y.; Mano, H.; Ogawa, S. Oncogenic mutations of ALK kinase in neuroblastoma. *Nature* **2008**, *455*, 971−974. (d) George, R. E.; Sanda, T.; Hanna, M.; Fröhling, S.; Luther, W.; Zhang, J.; Ahn, Y.; Zhou, W.; London, W. B.; McGrady, P.; Xue, L.; Zozulya, S.; Gregor, V. E.; Webb, T. R.; Gray, N. S.; Gilliland, D. G.; Diller, L.; Greulich, H.; Morris, S. W.; Meyerson, M.; Look, A. T. Activating mutations in ALK provide a therapeutic target in neuroblastoma. *Nature* **2008**, *455*, 975−978. (e) Eng, C. A ringleader identified. *Nature* **2008**, *455*, 883−884.
(10) (a) Shaw, A. T.; Solomon, B. Targeting anaplastic lymphoma kinase in lung cancer. *Clin. Cancer Res.* **2011**, *17*, 2081−2086. (b) Mosse, Y. P.; Wood, A.; Maris, J. M. Inhibition of ALK signaling for cancer therapy. *Clin. Cancer Res.* **2009**, *15*, 5608−5614.
(11) (a) Bossi, R. T.; Saccardo, M. B.; Ardini, E.; Menichincheri, M.; Rusconi, L.; Magnaghi, P.; Orsini, P.; Avanzi, M.; Lombardi Borgia, A.; Nesi, M.; Bandiera, T.; Fogliatto, G.; Bertrand, J. A. Crystal structures of analplastic lymphoma kinase in complex with ATP competitive inhibitors. *Biochemistry* **2010**, *49*, 6813−6825. (b) Lee, C. C.; Jia, Y.; Li, N.; Sun, X.; Ng, K.; Ambing, E.; Gao, M.; Hua, S.; Chen, C.; Kim, S.; Michellys, P.; Lesley, S. A.; Harris, J. L.; Spraggon, G. Crystal structure of ALK (anaplastic lymphoma kinase) catalytic domain. *Biochem. J.* **2010**, *430*, 425−437.
(12) Zou, H. Y.; Li, Q.; Lee, J. H.; Arango, M. E.; McDonnell, S. R.; Yamazaki, S.; Koudriakova, T.; Alton, G.; Cui, J. J.; Kung, P.; Nambu, M.; Los, G.; Bender, S. L.; Mroczkowski, B.; Christensen, J. G. An orally available small-molecule inhibitor of c-Met, PF-2341066, exhibits cytoreductive antitumor efficacy through antiproliferative and antiangiogenic mechanisms. *Cancer Res.* **2007**, *67*, 4408−4417.
(13) Kwak, E. L.; Bang, Y. J.; Camidge, D. R.; Shaw, A. T.; Solomon, B.; Maki, R. G.; Ou, S. H.; Dezube, B. J.; Jänne, P. A.; Costa, D. B.; Varella-Garcia, M.; Kim, W. H.; Lynch, T. J.; Fidias, P.; Stubbs, H.; Engelman, J. A.; Sequist, L. V.; Tan, W.; Gandhi, L.; Mino-Kenudson, M.; Wei, G. C.; Shreeve, S. M.; Ratain, M. J.; Settleman, J.; Christensen, J. G.; Haber, D. A.; Wilner, K.; Salgia, R.; Shapiro, G. I.; Clark, J. W.; Iafrate, A. J. Anaplastic lymphoma kinase inhibition in non-small-cell lung cancer. *N. Engl. J. Med.* **2010**, *363*, 1693−703.
(14) Pfizer Press Release, August 29, 2011.
(15) Galkin, A. V.; Melnick, J. S.; Kim, S.; Hood, T. L.; Li, N.; Li, L. Identification of NVP-TAE684, a potent, selective and efficacious inhibitor of NPM-ALK. *Proc. Natl. Acad. Sci. U.S.A.* **2007**, *104*, 270−275.
(16) (a) Katayama, R.; Khan, T. M.; Benes, C.; Lifshits, E.; Ebi, H.; Rivera, V. M.; Sharespeare, W. C.; Iafrate, A. J.; Engleman, J. A.; Shaw, A. T. Therapeutic strategies to overcome crizotinib resistance in non-small cell lung cancers harboring the fusion oncogene EML4-ALK. *Proc. Natl. Acad. Sci. U.S.A.* **2011**, *108*, 7535−7540. (b) Sakamoto, H.; Tsukaguchi, T.; Hiroshima, S.; Kodama, T.; Kobayashi, T.; Fukami, T. A.; Oikawa, N.; Tsukuda, T.; Ishii, N.; Aoki, Y. CH5424802, a selective ALK inhibitor capable of blocking the resistant gatekeeper mutant. *Cancer Cell* **2011**, *19*, 679−690. (c) Lovly, C. M.; Heuckmann, J. M.; deStanchina, E.; Chen, H.; Thomas, R. K.; Liang, C.; Pao, W. Insights into ALK-driven cancers revealed through development of novel ALK tyrosine kinase inhibitors. *Cancer Res.* **2011**, *71*, 4920−4931.
(17) Ott, G. R.; Tripathy, R.; Cheng, M.; HcHugh, R.; Anzalone, A. V.; Underiner, T. L.; Quail, M. R.; Lu, L.; Wan, W.; Angeles, T. S.; Albom, M. S.; Aimone, L. D.; Ator, M. A.; Ruggeri, B. A.; Dorsey, B. D. Discovery of a potent inhibitor of anaplastic lymophoma kinase with in vivo antitumor activity. *ACS Med. Chem. Lett.* **2010**, *1*, 493−498.
(18) Espinal, J. What is the role of the insulin receptor tyrosine kinase? *Trends Biochem. Sci.* **1988**, *13*, 367−368.
(19) Saltiel, A. R. Putting the brakes on insulin signaling. *N. Engl. J. Med.* **2003**, *349*, 2560−2562.
(20) Wan, W.; Albom, M. S.; Lu, L.; Quail, M. R.; Becknell, N. C.; Weinberg, L. R.; Reddy, D. R.; Holskin, B. P.; Angeles, T. S.; Underiner, T. L.; Meyer, S. L.; Hudkins, R. L.; Dorsey, B. D.; Ator, M. A.; Ruggeri, B. A.; Cheng, M. Anaplastic lymphoma kinase activity is essential for the proliferation and survival of anaplastic large-cell lymphoma cells. *Blood* **2006**, *107*, 1617−1623.
(21) There were 39 such structures with kinases like aurora kinase (3UNZ), ALK (2XB7), insulin receptor (3EKN), JNK1 (3ELJ), FAK (2JKK), ERk2 (2Z7L), CDK2 (1H01).
(22) Ott, G. R.; Wells, G. J.; Thieu, T. V.; Quail, M. R.; Lisko, J. G.; Mesaros, E. F.; Gingrich, D. E.; Ghose, A. K.; Wan, W.; Lu, L.; Cheng, M.; Albom, M. S.; Angeles, T. S.; Huang, Z.; Aimone, L. D.; Ator, M. A.; Ruggeri, B. A.; Dorsey, B. D. 2,7-Disubstituted-pyrrolo[2,1-*f*]-[1,2,4]triazines: new variant of an old template and application to the discovery of anaplastic lymphoma kinase (ALK) inhibitors with in vivo antitumor activity. *J. Med. Chem.* **2011**, *54* (18), 6328−6341.
(23) Selectivity value for 90% inhibition from single point data: $S(90)$ = (no. of kinases $\geq$ 90% inhibition)/(total no. of kinases tested).
(24) Cheng, M.; Quail, M. R.; Gingrich, D. E.; Ott, G. R.; Lu, L.; Wan, W.; Albom, M. S.; Angeles, T. S.; Aimone, L. D.; Cristofani, F.; Machiorlatti, R.; Abele, C.; Ator, M. A.; Dorsey, B. D.; Inghirami, G.; Ruggeri, B. A. CEP-28122, a highly potent and selective orally active inhibitor of anaplastic lymphoma kinase with antitumor activity in experimental models of human cancers. *Mol. Cancer Ther.* **2012**, *11*, 670−679.
(25) Pao, W.; Girard, N. New driver mutations in non-small cell lung cancer. *Lancet* **2011**, *12*, 175−180.
(26) Kraus, G. A.; Choudhury, P. K. Synthesis of purquinonic acid ethyl ester and deliquinone via a common intermediate. *J. Org. Chem* **2002**, *67*, 5857−5859.
(27) Yoshii, F.; Nakamura, T.; Hirono, S.; Shimizu, Y.; Hoshi, T.; Ando, M.; Hagiwara, H. Conformational analysis and selection of odor-active conformers: synthesis of molecules for the lily-of-the-vally (muguet)-type odor. *Helv. Chim. Acta* **2001**, *84*, 2051−2063.
(28) Goldberg, Y.; Bensimon, C.; Alper, H. Highly regioselective bromination of 2,3-dimethylanisole with *N*-bromosuccinimide. *J. Org. Chem.* **1992**, *57*, 6374−6376.
(29) Tolbert, L. M.; Haubrich, J. E. Photoexcited proton transfer from enhanced photoacids. *J. Am. Chem. Soc.* **1994**, *116*, 10593−10600.

(30) Angeles, T. S.; Steffler, C.; Bartlett, B. A.; Hudkins, R. L.; Stephens, R. M.; Kaplan, D. R.; Dionne, C. A. Enzyme-linked immunosorbent assay for trkA tyrosine kinase activity. *Anal. Biochem.* **1996**, *236*, 49−55.
(31) Rotin, D.; Margolis, B.; Mohammadi, M.; Daly, R. J.; Daum, G.; Li, N.; Fischer, E. H.; Burgess, W. H.; Ullrich, A.; Schlessinger, J. SH2 domains prevent tyrosine dephosphorylation of the EGF receptor: identification of Tyr992 as the high-affinity binding site for SH2 domains of phopholipase Cγ. *EMBO J.* **1992**, *11*, 559−567.
(32) Ghose, A. K.; Herbertz, T.; Pippin, D. A.; Salvino, J. M.; Mallamo, J. P. Knowledge based prediction of ligand binding modes and national inhibitor design for kinase drug discovery. *J. Med. Chem.* **2008**, *51*, 5149.